KERNFORSCHUNGSZENTRUM

KARLSRUHE

Oktober 1968

KFK 847
EUR 3721 e

Institut für Angewandte Reaktorphysik
Institut für Neutronenphysik und Reaktortechnik

Physics Investigations of Uranium-Fueled Fast Steam-Cooled Reactors in SNEAK, Assemblies 3A-0, 3A-2, 3A-3

Compiled by
R. Schröder

GESELLSCHAFT FÜR KERNFORSCHUNG M. B. H.

KARLSRUHE

KERNFORSCHUNGSZENTRUM KARLSRUHE

Oktober 1968

KFK 847
EUR 3721 e

Institut für Angewandte Reaktorphysik
Institut für Neutronenphysik und Reaktortechnik

Physics Investigations of Uranium-Fueled Fast Steam-Cooled Reactors in SNEAK, Assemblies 3A-0, 3A-2, 3A-3[1)]

Compiled by

R. Schröder

With contributions from

L. Barleon, R. Böhme, K. Böhnel, K. Burkart, M. Edelmann, P. Engelmann, G. Fieg, E.A. Fischer, G. Günther, F.W.A. Habermann[2)], E. Korthaus, D. Kuhn, W.Maier[3)], M.Müller, W.Oosterkamp[2)], A.M.Raberain[2)], H. Seufert, W. Seifritz, P. L. van Velze[2)], H. Walze, H. Werle, and D. Wintzer

Gesellschaft für Kernforschung mbH., Karlsruhe

1) Work performed within the association in the field of fast reactors between the European Atomic Energy Community and Gesellschaft für Kernforschung mbH., Karlsruhe

2) Euratom delegate

3) On leave from Allgemeine-Elektricitäts-Gesellschaft, Frankfurt

1. Introduction

Between May 1967 and March 1968 experiments on the SNEAK-3A series of assemblies have been performed, investigating the physics characteristics of fast steam-cooled uranium reactors of about 500 l core volume at operating steam density (see table 1). The steam was simulated by polyethylene foils. Two of the assemblies, corresponding to 40% (3A-1) and to 100% (3A-2) of the normal coolant density, have been investigated in considerable detail. Two more assemblies, investigated in less detail, have been obtained by voiding part of the core of assembly 3A-1 (viz. 3A-0) and by doubling the thickness of the polyethylene foils in part of the core of assembly 3A-2 (viz. 3A-3). The experiments done by end of September 1967, covering assembly 3A-1 and part of assembly 3A-0, have been reported and discussed previously /1/. This report covers the remaining experiments done at assembly 3A-0 and those done at assemblies 3A-2 and 3A-3. In some cases, a revised evaluation of 3A-1 experiments reported in /1/ will be given as in the meantime a more thorough evaluation could be done.

Many of the experimental data are of direct interest to the designer of a steam-cooled fast breeder reactor, e.g. the critical mass, the reactivity coefficient of the coolant density and the ratio of the capture rate of ^{238}U to the fission rate of ^{235}U as a function of position, that is closely related to the breeding ratio. Others, like the Doppler coefficient, are measured under conditions different from those in an actual fast reactor, but the comparison of experiment and calculation provides a valuable insight in the state of the art of calculating this effect.

All experimental results obtained were carefully compared with calculations with the intention to localize errors in the cross section sets used as well as to check the theoretical models applied.

Due to different hydrogen content, the four 3A assemblies cover a rather broad range of neutron spectra (see fig. 1). With increasing "softness" of the neutron spectrum, the influence of low energy resonance parameters of the reactor materials on integral data becomes more pronounced. Therefore, the theoretical analysis of the experimental results for the various assemblies is particularly suited to permit a judgement concerning the quality of different sets of group cross sections in this energy region.

Heterogeneity effects are also increasing with increasing hydrogen content of the assembly. The evaluation of the heterogeneity effects in those assemblies that have the softer spectra represents a rather severe test of the theoretical model applied. It was tried to perform the experiments in a way to separate heterogeneity and cross section effects.

A further object of study was the comparison of experimental and calculated reaction rate traverses near the core blanket interface.

The purpose of this report is to present a synopsis of the main results obtained rather than to cover the various experiments exhaustively. Some of the experiments have been evaluated in considerable more detail, and these results will be published separately.

2. Calculational Methods and Cross Section Sets Used

The Karlsruhe nuclear code system NUSYS has been applied to perform the calculations on an IBM-7074 computer.The following codes have mainly been used:

1) Normal one-dimensional diffusion calculation in cylinder and plate geometries.
2) One-dimensional diffusion calculation using an iterative, energy dependent buckling approach in successive problems of cylinder and plate geometries.
3) Two-dimensional diffusion calculation in R,Z and R,Θ geometries.
4) One-dimensional S4 calculation in cylinder geometry.
5) Cell calculations to obtain heterogeneity effects, using the ZERA code, described in /2/*.

In addition, different types of auxiliary codes were utilized to perform the evaluations.

The majority of calculations was performed using a 26 group structure**, however, for some of the two-dimensional calculations the respective 26 group sets were condensed to eleven groups.

---

* Due to a correction that had to be applied to the ZERA code, the results of heterogeneity calculations quoted in this report are not consistent with those for assembly 3A-1 given in /1/. The description of the ZERA program as such given in /2/ remains unchanged, however.

** The group structure is shown in fig. 1, for example.

The following cross section sets were used to perform the calculations:

1) The KFK-SNEAK set described in /3/. This set is being referred to as the normal SNEAK set, or SNEAK-NORM.
2) The KFK-SNEAK set with heterogeneity corrections applied. These corrections were obtained by use of the ZERA program, they are described in /2/. This set is being referred to asthe heterogenous SNEAK set, or SNEAK-HET.
3) The PMB set, also described in /3/. This set differs from the KFK-SNEAK set in two respects: First, ^{238}U capture data in the region from 10 keV to 800 keV have been slightly decreased, according to the data given by Pönitz et al. in /4/ and, secondly, ^{235}U capture and fission data in the region from 21.5 keV to 400 keV have been slightly decreased, leaving the ratio of capture to fission cross section unchanged.
4) The Russian cross section set described in /5/, referred to as ABN set.

There were no heterogeneity corrected versions of the PMB set and of the ABN set used. To clarify this, the suffix-NORM is occasionly attached to these sets.

3. Composition, Critical Mass and Effective Multiplication Factor

Fig. 2 shows the actual configuration of assembly 3A-2 as well as the dimensions used to perform the calculations. The cell structure of assembly 3A-2 is the same as described in /1/ for assembly 3A-1, with the only difference of an increased thickness of 0.5 mm for the polyethylene foils (see fig. 3). The average atom densities of the various zones of assembly 3A-2 as they were used for the homogeneous calculations are given in table 2 while table 3 lists the compositions of the platelets in the two core zones used for the cell calculations. The material of the subassembly tubes was smeared over the place occupied by the platelets. In a similar manner, the stainless steel of the steel frame for the polyethylene foil and the foil itself were homogenized for the calculation to give the composition of the platelet in question. The blanket was of uniform structure, therefore no heterogeneity-corrected cross sections had to be calculated.

The critical mass of the cylindrical reactor was experimentally determined as

$$M^K_{3A-2} = 400.3 \pm 0.9 \text{ kg } ^{235}U.$$

This value was corrected for irregular core periphery and for the fact that the core section of the regulating rod was not completely within the core. The critical volume corrected in the same way was found to be

$$V^K_{3A-2} = 505.3 \pm 1.4 \text{ l}.$$

Table 4 lists the results of k_{eff} calculations using the geometric data given in fig. 2 and the compositions mentioned before. The heterogeneity correction was found as the difference in k_{eff} due to two calculations using the SNEAK-HET set, first for the actual thickness of the platelets and secondly for this thickness reduced by the factor of 100. There are no S_4 corrections listed because our previous method to calculate these appears to have been inaccurate for small values of the correction.

Comparing the calculational results for k_{eff} of assembly 3A-2 with those for assembly 3A-1 shown in /1/, one finds the following trend: The cross section sets that have been used for both assemblies result in a lower k_{eff} for assembly 3A-2. In both cases, the k_{eff} values based on ABN cross sections are larger than unity, while the other results are smaller. For assembly 3A-1 the deviation between the calculated and the measured k_{eff} was largest for the calculation based on ABN data. The general trend to lower calculated k_{eff} values for assembly 3A-2, however, is in favor of the ABN based values. So, after applying the corrections for two dimensional calculations and for heterogeneity, the k_{eff} data based on the ABN or SNEAK set respectively disagree with the experimental value by about the same amount, but the deviation is in opposite direction.

The configurations of assemblies 3A-0 and 3A-3 are shown in figures 4 and 5. The composition of the void zone in assembly 3A-0 is equal to that of the central zone of assembly 3A-1 (see tables 1, 2 in /1/) with all hydrogen and the corresponding amount of carbon removed. The composition of the central zone of assembly 3A-3 is equal to that of the central zone of assembly 3A-2 with the hydrogen concentration doubled and with the corresponding amount of carbon added.

4. Investigation of the Coolant Reactivity Coefficient

4.1 Kind of Experiments

To obtain an insight in the accuracy of predicting the dependence of reactivity on coolant density for steam-cooled fast breeder reactors a set of three experiments was performed, viz.:

1) Voiding various core zones in assembly 3A-1;
2) Same in assembly 3A-2;
3) Flooding various core zones in assembly 3A-2.

Voiding was achieved by removing the polyethylene foils from the steel frames for the volume considered while the flooding effect was simulated by doubling the thickness of these foils. The assembly was kept critical by exchanging core-elements for blanket-elements or vice versa. The error attached to the experimental reactivity values amounts to about ±5%.

4.2 Method of Calculation

The calculations performed use one-dimensional diffusion theory for changes of the polyethylene density in the core, that are symmetric with respect to the core axis. For experiments that involve either sector-shaped zones or simultaneous changes of the polyethylene density in the core and in the axial blanket, two-dimensional diffusion theory was applied.

Fot the one-dimensional calculations the bucklings of the separated direction were either gained by fitting a cosine to the axial fission rate distribution of ^{235}U that was found experimentally (3A-1), or the energy dependent bucklings of the unperturbed system obtained by iteration of successive radial and axial calculations were used (3A-2). The one-dimensional calculations were performed using the normal 26 group structure. For the two-dimensional calculations the 26 group set was condensed to 11 groups. The majority of results reported is based on the SNEAK-HET set.

To get an impression concerning the influence of heterogeneity effects, the calculations based on the SNEAK set were performed for the actual thickness of the platelets as well as for the thickness reduced by the factor of 100. It was found, that the heterogeneity correction increases the calculated reactivity effect by the order of 4 to 10%, and in doing so gives a result closer to the experiment.

There is an error of about ±5% assigned to the calculational results quoted in this section. This is partly due to a temporary error in the ZERA code, mentioned before, that affected the preparation of heterogeneity-corrected cross sections. Control calculations done with the corrected ZERA code led to the magnitude of the error.

4.3 Results and Discussion

4.3.1 Void Experiment in 3A-1

First, a central zone of variable height was voided and, subsequently, a sector-shaped zone. Fig. 6 shows the various steps, step 4 leading to assembly 3A-0. Table 5 lists the reactivity effects found by experiment and by calculation.

There exists a discrepancy between experiment and calculation of about 12% for larger voided zones and 15% for a smaller central void. The discrepancy is reduced to about 5% if the PMB set is used. Results based on the ABN set, however, are low by about 35%.

4.3.2 Void Experiment in 3A-2

In this experiment, the polyethylene foils were removed in a smaller central zone only (see fig. 7). A special feature of this experiment was an investigation of the influence of the blanket on the void effect. Therefore, the metallic uranium blanket containing no polyethylene, that is normally used in SNEAK, was partially exchanged with a uranium-oxide blanket containing polyethylene. This results in a more realistic simulation of an actual breeder blanket. The composition of this blanket is shown in table 6. The exchange was done for the axial blankets of the

nine central and of the twelve adjacent elements. Table 7 lists the results of experiment and calculation. It is found, that the influence of the breeder blanket is rather small: It has no influence on the central void effect at all, while the effect of voiding the axial blanket of the central zone in addition to the respective part of the core amounts to only 1.5% of the core effect.

The agreement between experiment and SNEAK-HET calculations is slightly worse than it is for the void experiment in 3A-1, the discrepancies vary from 13% to 17%.

4.3.3 Flooding Experiment in 3A-2

By doubling the thickness of the polyethylene foils a steam density in the coolant channels of about 0.15 g/cm^3 (see table 1) was simulated. First, the foil thickness in the central zone was increased for zones of different height and then the radial effect was investigated by "flooding" a sector, see fig. 8. The results are shown in table 8. The discrepancies between experiment and calculation are in the range from 18% to 24%, they are the largest of all experiments of this type.

4.3.4 Coolant Reactivity Coefficient

From the void and flooding experiments in SNEAK-3A-2 the reactivity coefficient of coolant density can be obtained as $\frac{\Delta k}{k}/\frac{\Delta \varrho}{\varrho}$ = +0.053* for the steam density simulated by assembly 3A-2. Calculations using the SNEAK and ABN sets result in values of 0.047 and 0.040 respectively /6/.

4.3.5 Conclusions

In concluding, it can be said that the magnitude of the reactivity effect of changes in steam-density is predicted too small by calculations for density changes in either direction. The discrepancy is of the order of 15% to 25% increasing with the hydrogen concentration. Calculations using the ABN set give values that are low by 30 to 35% at all hydrogen concentrations. A more detailed evaluation of these experiments is presented in /6/.

---

* ϱ steam density

5. Investigation of Heterogeneity Effects

The importance of heterogeneity effects for the interpretation of nearly all experiments requires a good understanding of the respective effects in different energy ranges. A combined investigation of integral (reactivity) and differential (flux fine structure at different energy ranges) effects of the heterogeneous core structure in different spectra is a sensitive test of the theoretical model, that forms the basis of the cell program ZERA /2/.

5.1 Reactivity Effects

For these reasons, the series of heterogeneity experiments, which was started in SNEAK-3A-1 /1/, was continued in assembly 3A-2. The softer spectrum in assembly 3A-2 causes higher heterogeneity effects in the low energy range ($E < 20$ keV) of the neutron spectrum, while the high energy contributions are nearly the same as in 3A-1.

5.1.1 Experimental Procedure

As in assembly 3A-1, the normal cell structure of a series of fuel elements was changed to "single-bunched" and in a second step to "double-bunched" cells (see fig. 10). The mean composition of the fuel elements was the same in all three cases. Reactivity changes due to bunching were obtained from critical control rod positions. Bunching of cells was performed in test regions of different radial position, which are indicated in fig. 10. The dependence of reactivity effects due to bunching on the axial position of bunched cells was investigated in the central test region 1. In all experiments, the location of the bunched cells was symmetrical with respect to the midplane of the core. In this way, linear reactivity effects due to displacement of fuel platelets within the elements have been avoided.

5.1.2 Methods of Calculation

Calculated reactivity effects due to bunching have been obtained in 3 steps:

1) Calculation of heterogeneity corrected cross sections for normal, single, and double-bunched cells, using the cell program ZERA.
2) One-dimensional 26 group diffusion calculations for the assembly with normal core cells.
3) Perturbation calculations with cross sections for single-and double-bunched cells.

5.1.3 Results and Discussion

5.1.3.1 Experiments in the Central Test Region 1

The measured reactivity effects, caused by single-and double-bunching in the central test region are plotted in fig. 9 as a function of the bunched fraction of core height. The experimental values contain small ($\approx 1\%$) corrections for second order effects of fuel displacement. For comparison, the corresponding reactivity effects measured in assembly 3A-1 are shown in the same figure.

Generally, the measured bunching effects are by about 15% larger than the calculated ones. Since the calculations do not include axial (perpendicular to the plate surfaces) leakage changes, the reasonable agreement between experimental and calculated values confirms that the bunching effects in test region 1 are mainly due to an increased ratio of fissions to absorptions. Radial leakage effects are small in this test region.

The reactivity effects due to bunching in test region 1 are by a factor of about 1.5 to 1.7 higher than those in assembly 3A-1. The higher values are partially caused by the smaller core radius of assembly 3A-2. The remaining difference in the central bunching effects is caused by increased heterogeneity effects in the softer 3A-2 spectrum.

5.1.3.2 Bunching Effects at Different Radial Element Positions

The experimental results of single and double bunching over the full height of the core are shown in fig. 11 as a function of radial position of elements with bunched cells. The agreement between measurement and calculation in the shape of the curves and in absolute values is quite satisfactory. Again, the calculations underestimate the effect. The discrepancy amounts to about 15% near the core center. The change in sign of the effects near the blanket due to increased diffusion coefficients in the bunched cells is well described by the calculations, however.

5.2 Fine Structure Effects

5.2.1 Fine Structure within the Unit Cell

For the double-bunched states of assemblies 3A-2 and 3A-3 traverses over the unit cell were measured with four types of activation detectors. These detectors were selected to give information concerning the local variation of the neutron flux within a small energy band. Three of the detectors were identical to those used to determine the neutron spectrum with the sandwich foil technique and this technique*) was also applied. The forth detector, a rhodium foil, makes use of the Rh(n,n') reaction. The sandwich detectors have more than one resonance and the corresponding results were reduced to the main resonance energy making use of resonance parameters and of the spectrum calculated by the ZERA program. In this way the local flux variations at 577 eV, 18.8 eV,and 4.9 eV have been determined. The rhodium activity is mainly (≈70%) due to the energy range between 800 keV and 4 MeV, although its threshold energy amounts to 40 keV.

The local flux variations determined experimentally are shown in figures 12 and 13 that present also the results of calculations. For rhodium, the local fluxes for the corresponding energy groups have been averaged according to the energy dependence of the activation cross

*) for details see chapter 6.2

section. The calculational results shown in these figures are based on the ZERA program.

The agreement between experiment and calculation is quite reasonable in the majority of the cases. For assembly 3A-2, the experimental rhodium activation curve and the experimental flux curve for the copper resonance show a more pronounced local oscillation than the corresponding curves calculated. The deviations are smaller for the tungsten and gold foils. The discrepancy between experiment and calculation is more pronounced in assembly 3A-3. While for rhodium the discrepancies are only slightly larger, the local fluxes at the resonance energies of copper and gold show less agreement between experiment and calculation than they do for assembly 3A-2. For tungsten the discrepancies are rather small again.

At present, these deviations are not understood. It is quite possible that they can be traced to errors in the cross sections used to determine the local flux variation.

5.2.2 Fine Structure within the Fuel Platelets of the Unit Cell

The fine structure of the fission rates of ^{235}U and ^{238}U and of the capture rate of ^{238}U within the fuel platelets was determined experimentally (see fig. 14) for the double-bunched assemblies 3A-2 and 3A-3 and was compared with theory. This is a very rigid test of the ability to calculate heterogeneity effects. The experiment was performed using 0.1 mm thick uranium foils of .4% and 20% enrichment. About five experimental points were established over the fuel zone that had a thickness of 1.26 cm. The fuel zone was built up of platelets of 3.14 mm thickness for this experiment. The calculations were carried out with the aid of the ZERA program.

As can be seen from figure 14, the relative spatial behavior is calculated quite well for the fission rate and the capture rate of ^{238}U, while the fission rate of ^{235}U shows a flatter behavior by calculation than by experiment. This was found already for assembly 3A-1 /1/.

The discrepancy may be due to incorrect cross sections or to a deficiency of the method of calculation. Because two of the three experimental results compare quite favorably with the calculation, the first conclusion seems to be more likely. In this context, however, one also has to realize that the gross local variation of the fission rate of ^{235}U is the sum of two contributions of opposite sign from the fission energy range and from the range of resonance energies.

The fine structure of the rates mentioned above was also determined for the standard cell structure and for the single-bunched cell. Fig. 15 shows the average values of the central reaction rate ratios that can be found from these data for the various degrees of bunching.

A detailed discussion of the central reaction rate ratios for the standard cell structure is presented in chapter 8.1.

5.3 Spectrum Effects

For assemblies 3A-2 and 3A-3 the neutron spectrum in the aluminum platelet was determined for the normal cell structure and for the double-bunched state in the energy range below 3 keV by means of the sandwich foil method.*) The experimental method and the results of spectrum measurements for the normal cell structure in all assemblies will be discussed in chapter 6.2.

The results of measurement and calculation agree within the experimental error limits for the normal as well as for the double-bunched state of assembly 3A-2. For assembly 3A-3, however, there seems to be an indication of less measured than calculated neutrons around 400 keV**) for the double-bunched state. While for the normal state one still can just state agreement within the experimental error limits, the three data points in question are also situated below the calculated curve. In the assemblies to follow, this effect will be further investigated, as in the meantime it will be possible to reduce the experimental error considerably.

---

*) see fig. 16

**) for normalization of data see chapter 6.2.

6. Neutron Spectrum

The proton recoil spectrometer technique was used to cover the energy range from 10 keV up to 1.1 MeV. In the lower energy field the spectrum was determined for 10 energies ranging from about 1.5 eV to 3 keV by means of the foil activation technique.

6.1 Proton Recoil Spectrometer

The measurements were performed using spherical proportional counters. The energy range from 30 keV to 600keV was covered by three counters using hydrogen of 1, 2, and 4 atm. pressure respectively, while a counter filled with 2.5 atm. of CH_4 served to cover the range from 400 keV to 1.1 MeV. The data were corrected for wall effects /7/. In the energy range below 40 keV, the γ-n discrimination technique described by Bennet /8/ was applied. To accomodate the counter and its pre-amplifier, platelets were removed from one drawer for a distance of about 30 cm. The majority of measurements was done with the reactor being critical. Some of them, however, were performed at up to 5% subcriticality.

A comparison of measured and calculated neutron spectra for the core center of assemblies 3A-0, 3A-2, and 3A-3 and for a blanket position of assembly 3A-2 is given in figures 17 to 20. The experimental data were integrated to give group fluxes. The comparison is made for groups 6 to 11 covering the energy range from 10 keV to 800 keV. Group 5 was not included because the experimental data cover only part of the corresponding energy range. The error of about $\pm$15% assigned to the data for energies below 40 keV is mainly due to problems related to the γ-n discrimination. The comparison was done by normalizing all spectra (measured or calculated) to equal area below the curve for groups 6 to 11. For assembly 3A-2 a comparison with the results of diffusion calculations using different sets of group-constants was made while the others are just compared with calculations based on the SNEAK-NORM set.

There is not much difference in the results of calculations using the SNEAK-NORM set, the SNEAK-HET set, and the PMB set. The results based on the ABN set, however, differ quite markedly from the others.

Considering first the spectrum in the core center of assembly 3A-2, the calculations based on the SNEAK set and on the PMB set show too few neutrons on the high energy side (group 6) and too many neutrons on the low energy side (groups 9 to 11) of the maximum, so resulting in a slight shift of the maximum to lower energies. The calculations based on the ABN set show a somewhat opposite behavior.There are too many neutrons in group 6, and too few in groups 7 to 9. For the remaining two groups, however, i.e. below 46 keV, the ABN set also results in too many neutrons as does the SNEAK set. The disagreement between experiment and calculation is qualitatively very similar for all the assemblies, the only exception being the rather large deviation in group 10 for assembly 3A-0.

Considering now the spectrum in the blanket, the SNEAK set and the PMB set result in too many neutrons on the high energy side while the ratio of calculated to experimental flux is somewhat oscillating around 1.0 for the lower energies. The ABN set also results in too many neutrons on the high energy side, as it does in the core, followed by too few neutrons below. For all sets, the agreement with the experiment in the energy range from 10 keV to 40 keV is much better in the blanket than in the core.

6.2 Resonance Activation Foils in Sandwich Geometry

As compared to the measurements done at assembly 3A-1, four foil materials were added (see table 9). The foils were of 1.8 cm diameter, the sandwich was irradiated inside a cadmium box of 0.5 mm thickness. To produce results directly comparable with calculations of spectra for a heterogeneous cell structure, one sandwich each was placed within the aluminum platelet of the unit cell that had a small cavity provided for this purpose. Foils of different materials were irradiated at the same time in equivalent aluminum platelets of different cells along the cylinder axis. The greatest distance from core center did not exceed 20 cm.

All activities were converted to activity at the core center by calculation. Differences in core spectrum along the axis were found to contribute very little compared to other sources of errors associated with this method and, therefore, were neglected.

To either determine or re-check the calibration factors that depend on counter efficiency, the irradiation of all foil materials was repeated in an 1/E spectrum. In addition, an irradiation was performed in a fast uranium graphite system built up in the Karlsruhe fast subcritical facility SUAK. The corresponding spectrum had been determined by the time-of-flight technique. This spectrum, naturally, is quite closer to the spectra investigated in the SNEAK-3A assemblies than is the 1/E spectrum. This calibration was done for ^{23}Na, ^{63}Cu, ^{98}Mo, ^{55}Mn, ^{114}Cd, ^{81}Br, and ^{197}Au.

The evaluation was done using the TRIX-1 program. The data for the resolved as well as for the unresolved resonances were taken from /9/. The spectra of the different SNEAK assemblies needed for the calculation of contributions due to higher and unresolved resonances were found using the ZERA code based on SNEAK set cross sections. Figures 21 to 23 show the central core spectra of SNEAK assemblies 3A-0, 3A-1, 3A-2, and 3A-3. The results for assembly 3A-1 replace the preliminary results for this assembly given in /1/. The differences are due to recalibration of foils and to effects of unresolved resonances that had not been considered before. The experimental error margins given for flux values are composed of the following contributions:

1) Counting statistics (order of magnitude 5%);
2) Foil weight (order of magnitude 1%);
3) Local variation of foil thickness (order of magnitude .1%);
4) Instability of electronic equipment (order of magnitude 2%);
5) Correction for foil position along the axis (order of magnitude .1%)
6) Spectrum used to correct for activities not related to the main resonance (order of magnitude 5%);
7) Resonance parameters (order of magnitude 5% to 10%);
8) Foil positioning (order of magnitude 1%);
9) Calibration factor (order of magnitude 5% to 10%).

The calculational results shown in figures 21 to 23 were obtained by means of the ZERA code using the SNEAK cross section set. The flux spectrum shown is that within the aluminum platelet. For comparison with experimental data, the step curve calculated was smoothed by connecting adjacent steps by a straight line in the figures. One has to keep in mind, however, that the actual spectrum shows dips at the resonance

energies of ^{238}U. It was checked that no overlap between a foil resonance and a resonance of ^{238}U exists in the energy range below 100 eV.

The normalization of experimental to calculated values shown in figures 21 to 23 was selected to give best agreement between the experimental and the calculated curve over the energy range in question. At present, the experimental values of the spectrum determined by the sandwich method are not to the same scale as those determined by the proton recoil method, and the scaling factor is unknown. For the future measurements this factor will be known, following an absolute determination of foil activities.

For the normalization chosen, the calculated spectra agree with the experimental ones within the experimental error limits in the whole energy range covered by sandwich foils for all the four assemblies.

7. Neutron Importance

The space and energy dependence of the neutron importance $\phi^+(\underline{r},E)$ has been investigated in SNEAK assembly 3A-2 using the neutron sources ^{252}Cf, Am/Be, Am/B, Am/F, Am/^{10}B, Am/Li, and Sb/Be. If a neutron source with source strength S and energy spectrum f(E) is placed in a reactor at position $\underline{r}$, the effective source strength that enters the kinetic equations will be given by

$$S \int_0^\infty f(E)\phi^+(\underline{r},E)dE.$$

This quantity was determined experimentally by an analysis of the time behavior of the reactor power before and after a reactivity step of known magnitude (-20¢) was introduced. The kinetic equations were solved in an iterative way.

To compare an effective source strength measured with the corresponding value calculated, the source spectrum f(E) and the source strength S have to be known. It is sufficient, however, to know S on an arbitrary scale, that is the same for all sources considered. The energy

spectra were taken from /10/ to /16/. As there is no information available concerning the three americium sources Am/B, Am/^{10}B, and Am/F, the spectra of the corresponding polonium sources were used. Considering that the α-energies of Am (5.48 MeV) and Po (5.3 MeV) are rather close to each other, this was thought to be a reasonable approximation. The spectra actually used for the evaluation are shown in fig. 25. An experimental determination of the spectra of all neutron sources used for these measurements will be done in the near future. The source strengths S were determined relative to each other in a manganese sulfate bath.

Table 10 shows the results of experimental and calculated effective source strengths for the center of SNEAK assembly 3A-2. The adjoint fluxes were taken from a 26 group diffusion calculation based on the SNEAK-HET set as shown in fig. 24. The source strengths are normalized to that of ^{252}Cf. First, it can be seen from table 10 that the general agreement between experiment and calculation is quite good. On the other hand, there appears to be a trend to higher experimental than calculated values towards lower energies for the normalization chosen. The experimental value for the Sb/Be source, corresponding to an energy of 24 keV, is higher than the calculated one, the experimental error limits of this value are $\pm$1.5%, while the discrepancy with the calculated value amounts to 5.5% for the SNEAK-NORM set and to 3.5% for the ABN-NORM set. This trend may indicate that the ratio of macroscopic absorption to fission cross section of the core mixture in this energy range or slightly below is smaller than it is assumed for the calculations.

In this context one also has to recall, however, that the procedure to obtain the group cross sections of the SNEAK set uses a weighting spectrum that is rather different from the adjoint spectrum. This effect will be further investigated.

The radial dependence of the effective source strength of the various sources is shown in fig. 26. The general agreement between experiment and calculation is quite good. On the other hand, some of the experimental values appear to lie below the calculated curve close to the core-blanket interface, if both sets of values are normalized at the core center. This behavior is particularly expressed by the traverse associated with the Am/Li source. These deviations will be further studied.

A more detailed discussion of the experiments concerning neutron importance is in preparation.

8. Reaction Rates

Various reaction rates and their ratios were determined as a function of position by foil activation and with fission chambers.

8.1 Reaction Rate Ratios for the Core Center

8.1.1 Foil Measurements

The fission rates of ^{235}U and ^{238}U and the capture rate of ^{238}U were determined by the foil activation technique as a function of position within the unit cell. To perform these measurements, 0.1 mm thick uranium foils of 2.54 cm diameter were used, they were of .4% and of 20% enrichment. Two foils of each enrichment were irradiated at the same time in each position. These pairs of foils were usually placed between two platelets. To obtain experimental results for positions within a fuel platelet, special platelets with a central cylindrical hole were fabricated to accomodate the foils. The space between two pairs of foils was filled with uranium discs of 20% enrichment. The absolute ^{238}U capture rate was determined using the method described in /17/ while the fission rates were determined by counting the fission product γ-activity above 662 keV. An absolute calibration of the fission rates was achieved by irradiating a pair of foils closely attached to an absolutely calibrated fission chamber. Fig. 27 shows the space dependence of the reaction rate ratios for assembly 3A-2. Even for the normal structure of 1.26 cm thickness of the unit cell, the spatial variation of the rate ratios is not negligible. The experimental data shown in table 11 for assembly 3A-2 are the ratios of the reaction rates that have been averaged over the fuel plate of the unit cell. Table 11 also presents the corresponding calculated values that are based on rate calculations for the fuel plate using the ZERA program. The spectral index $(\sigma_f{}^{238}U)/(\sigma_f{}^{235}U)$ is underestimated by all cross section sets used. The deviation ranges from 13% for the SNEAK set to 11% for the ABN set. The spectral index $(\sigma_c{}^{238}U)/(\sigma_f{}^{235}U)$ is underestimated by the ABN set by 6% while the other sets overestimate this value by about 5%.

8.1.2 Fission Chamber Measurements

Although it seems very reasonable to consider the local variations due to fine structure effects, the fission chamber measurements were also continued to obtain a consistent set of fission rate ratios for all the SNEAK-3A assemblies investigated. These chambers were placed in small cavities, they cannot give an exact information concerning reaction rates in the fuel platelets. The results of experiment and calculation for assemblies 3A-0, 3A-2, and 3A-3 are shown in tables 12, 11, and 13. While the calculated values for the reaction rate ratios of assemblies 3A-0 and 3A-3 are based on the normal SNEAK set, the values concerning assembly 3A-2 were calculated using the various cross section sets considered in this report. There is little difference between the results based on the SNEAK set either heterogeneity-corrected or normal. The fission rate ratios of ^{238}U, ^{233}U, and ^{239}Pu to ^{235}U are best described by the ABN set while for the fission ratio of ^{232}Th to ^{238}U the SNEAK and PMB sets give better results.

8.2 Traverses of Reaction Rates and Their Ratios

8.2.1 Foil Measurements

To ensure that traverses of reaction rate ratios are not influenced by fine structure effects, the two ratios $\sigma_c^{238}/\sigma_f^{235}$ and $\sigma_f^{238}/\sigma_f^{235}$ were determined by the foil activation technique as a function of position within the unit cell for two core locations. One of these was at the core center while the ohter was close to the core blanket interface. There was no difference found in the relative local variation of the

spectral indices for the two locations. Therefore the reaction rates could be determined within the aluminum platelet of the unit cell. These values were used to obtain traverses of reaction rate ratios and of the reaction rates themselves.

The experimental and calculated reaction rate ratios along the cylinder axis measured by foil activation are shown in fig. 28. As mentioned before, the central ratio of capture rate in ^{238}U to fission rate in ^{235}U is overestimated by the calculation based on the SNEAK set by about 6%, while it is underestimated by the calculation based on the ABN set by the same amount. These deviations are practically constant over the core region. Proceeding into the blanket, the theoretical overestimation based on the SNEAK set changes to an underestimation at about one third of the blanket thickness. This deviation then increases rather rapidly towards the blanket edge. The calculation based on the ABN set gives too low results all over the blanket, but the discrepancy increases towards the core edge. Concerning the ratio of fission rates of ^{238}U to ^{235}U, the calculation based on the SNEAK set underestimates this quantity constantly by about 14% across the main part of the core. The agreement in the blanket however, is very good, deviations close to the reactor edge are of no significance due to experimental uncertainties. The ABN set gives a rather similar result, in the core the underestimation is slightly smaller (12%), while in the blanket the agreement is not quite as good as for the SNEAK set.

The three experimental traverses of the reaction rates themselves were also compared with the calculated ones for the core and the blanket region. In fig. 29 experimental and calculated results are normalized at the center, the scales shown in the figure are arbitrary. While the deviations between experiment and calculation are comparatively small in the core region, they become quite large immediately behind the core blanket interface. The curve for the fission rate of ^{238}U in particular shows a very pronounced step at the core boundary. While the detailed behavior of the deviations is different for the curves based on the SNEAK set and the ABN set, the principal discrepancies are the same. One has to conclude that close to the core blanket interface the actual reaction rates are higher than the calculated ones if the normalization is made at the core center.

The experimental traverses within the inner core region were fitted by a cosine function cos Bz within z = ±34 cm from the midplane. The equivalent procedure then was applied to the traverses based on one-dimensional diffusion theory or S4 calculations. It may be mentioned, that the parameter B depends slightly on the distance from the midplane that is used for the fitting process. The bucklings B^2 obtained in this way are shown in table 14. All the experimental bucklings are lower than the corresponding ones calculated by diffusion theory. Comparing the experimental values with S4 calculations, however, leads to good agreement for the fission rate traverse of ^{238}U, while the discrepancies for the two other rates remain about the same. The remaining discrepancies can be due either to a relatively lower calculated neutron population towards the core edge or to a systematic error in reaction cross sections that increases towards the core edge. The latter may be due to change in spectrum and to incorrect calculation of self-shielding.

The axial traverses for the fission rate of ^{235}U and the capture rate of ^{238}U were integrated in z direction of the reactor. Combined with the central reaction rate ratios, they result in a quantity that is related to the initial breeding ratio, defined as

$$IBR = \frac{^{239}Pu \text{ produced}}{^{235}U \text{ consumed}} = \frac{\text{Integrated capture rate of } ^{238}U}{\text{Integrated absorption rate of } ^{235}U}$$

$$= \frac{\text{Integrated capture rate of } ^{238}U}{\text{Integrated fission rate of } ^{235}U} \times \frac{1}{1 + \frac{\text{integrated capture rate of } ^{235}U}{\text{integrated fission rate of } ^{235}U}}$$

A comparison of experiment and calculation for the first factor of the last expression, integrated in direction of the cylinder axis only is shown in table 15. The diffusion theory calculation leads to an overestimation of this quantity by the SNEAK NORM and the PMB NORM sets between 3 and 4 percent, while the ABN set results in an underestimation of about 4%. Comparing these data with the results of k_{eff} calculations (see table 4) one will note the correlation between a low value for

the ratio of the integrated reaction rates and a high value for k_{eff}. Table 15 also gives the core and blanket contributions to the reaction rate integrals.

The results of the foil activation experiments are discussed in more detail in /18/.

8.2.2 Fission Chamber Measurements

In addition to the foil measurements, small fission chambers were used to determine central axial traverses for ^{235}U and ^{239}Pu. These chambers could be moved within a tube of 17 mm by 17 mm cross section placed inside a SNEAK element. The rest of the element was filled with SNEAK platelets standing upright, some of them of smaller size than normal. In this way the void volume was minimized, the platelets were of an average composition very close to that of the core zone. Immediately below the upper blanket, an aluminum zone of 37 mm thickness had to be introduced.

The two experimental traverses along the core axis again were compared with the corresponding ones calculated, the results are shown in fig. 30, experimental and calculated curves are normalized in the center. The two traverses behave very similar. The dip close to the upper blanket is thought to result from the additional aluminum zone, mentioned before. The fission rate traverse of ^{235}U obtained by chamber measurements does not agree with the one based on foil activation. In the core, the chamber traverse is flatter than the foil traverse and that again is flatter than the calculated one, this behavior is also expressed by the different experimental bucklings of tables 14 and 16. In the blanket, however, the discrepancies become more pronounced. For the normalization chosen, the chamber traverse results in about 20% more neutrons than the foil traverse in the inner half of the blanket. Further out, a comparison is not possible due to bad statistics. The additional neutrons found by the chamber traverse may be due to streaming effects through the guide tube.

The traverses were also fitted to a cosine function, the values for z = ±25 cm from the core midplane were used in this case, they are shown in the first line of table 16. The values for the ^{235}U and the ^{239}Pu traverse are very close to each other. The experimental buckling based on the ^{235}U fission rate traverse is about 6% smaller than the equivalent value found by foil measurements.

Fission chamber traverses for ^{235}U, ^{239}Pu, ^{238}U and ^{237}Np were also measured parallel to the cylinder axis for different positions in core and blanket, i.e. for different distances from the central axis. The different positions were selected along X = 19, with one exception. Because the measurements done at position 19/16 have been influenced by a He chamber that was in the reactor for other experiments, a traverse was also done along position 22/18 being at a similar distance from the center axis.

Table 16 shows the results of fitting a cosine to the experimental points that are within ±25 cm of the horizontal midplane of the assembly. The bucklings related to the fission rate traverses of ^{235}U and ^{239}Pu show an increase of about 8 to 9% from the central traverses to the one most remote from the center. For the same radial position, the experimental bucklings related to ^{235}U and ^{239}Pu agree very well. The rate traverses for ^{238}U and ^{237}Np were not measured over all the radial positions, but assuming the same behavior of the traverses for both of these threshold reactions results in a less pronounced increase of the buckling for the outer traverses.

The experiments show that the reaction rates are not strictly separable in the radial and axial direction.

9. Material Worth Measurements

9.1 Central Material Worths

9.1.1 Experimental Procedure

Central reactivity worths for a number of samples were measured in all assemblies using the horizontal drawer and the sample changer. The samples were investigated either within an empty sample box or within a sample box filled with core material.

The experimental reactivity worths were determined using the inverse kinetic program with a correction apllied for the transport of precursors by the sample changer. The results were also corrected for linear reactivity drift between two reference measurements. The experimental errors are mainly caused by non-linear temperature drift effects. The composition of the fuel samples is shown in table 17.

9.1.2 Method of Calculation

The central reactivity worths have been calculated by perturbation theory applied to results of one-dimensional diffusion theory in cylinder geometry. Within the perturbed zone of 1 cm^3 volume a small amount of the sample material was added to the core mixture. It is realized, that a more appropriate treatment has to consider the heterogeneous core structure of the sample environment and self-shielding effects within the sample. An evaluation of material worth measurements that will consider these effects is in preparation. For all assemblies, the SNEAK-NORM set was used for the calculation, while, in addition, for assemblies 3A-1 and 3A-3 results based on the ABN set are reported.

9.1.3 Results and Discussion

Table 18 lists the central reactivity worths for all the 3A assemblies while table 19 gives the ratios of calculated to measured values. The experimental rate and material worth traverses generally

showed a flatter behavior than the calculated ones. In case this is due to a flatter flux distribution than calculated, this will result in a higher normalization integral for the perturbation calculations. An estimate showed this effect to result in a probable increase of about 5% for the normalization integral, i.e. a decrease of 5% in reactivity values. This correction has not been applied to the values listed in tables 18 and 19.

The change of the material worths of a certain sample in the different assemblies is in part due to spectral effects on the sample material itself. In addition, the normalization integral changes, mainly due to smaller core sizes of those assemblies that have softer spectra. This tends to increase the absolute values of the material worths of all samples with increasing hydrogen content of the core.

9.1.3.1 ^{235}U

All experimental values are smaller than the corresponding calculated ones by about 10 to 20%. This is in favor of ABN based data, that result in smaller values of the material worths than the data based on the SNEAK set.

9.1.3.2 ^{238}U

The sample size effect can be judged best from measurements in assembly 3A-2. The environmental effect results in values by 10 to 15% higher in the void environment. Taking the average of the experimental results for the smallest sample in both environments one estimates that the absolute reactivity is calculated by about 15% too large, i.e. too negative, in case the SNEAK set is used. Results based on the ABN set are wrong by about 7% in the other direction.

9.1.3.3 ^{239}Pu

The data available do not allow any judgement concerning the sample size effect. The environmental effect has been determined for the largest sample only, it amounts to between 2% (3A-0) and 6% (3A-2). The value associated with assembly 3A-3 was determined using the smallest sample and therefore is considered to be the most reliable one. It is in good agreement with calculations based on ABN set data, while data based on the SNEAK set are low by 8%. For all the other assemblies, results for larger samples are available only. In these cases the calculations based on the SNEAK set as well as those based on the ABN set result in data that are too high. This is possibly due to the sample size effect.

9.1.3.4 ^{10}B

The sample size effect is very pronounced, it has been investigated in assembly 3A-2, in particular.The environmental effect appears to be negligible. The reactivity worth associated with the smallest sample results in good agreement between experiment and calculation based on the SNEAK set for assembly 3A-2, while there is a slight underestimation of 4% by the respective calculation for assembly 3A-0. For the other assemblies, data for the smallest sample are not available.

9.1.3.5 CH_2

Both sets of cross sections lead to results too low by about 20 to 35% depending on assembly and sample environment.

9.1.3.6 Note Concerning Degradation Effects

If the reactivity effect of a material is either completely or at least substantially due to degradation effects, the calculated reactivity worth is very sensitive to small errors in the energy distribution of importance. Starting from high energies, the importance first decreases, having a minimum at about 1 MeV (see fig. 24).

Proceeding to lower energies, the importance than is slowly increasing to about 1 keV. The first decrease will result in a negative degradation effect and the subsequent increase in a positive one. Therefore, the net effect is a sum of two contributions of opposite sign.

9.1.3.7 Reduction of Self-Shielding

For materials showing a rather small reactivity effect, a reasonable contribution may be due to reduction of self-shielding effects in the surrounding core material. Perturbation theory is inadequate to calculate this effect correctly. A better treatment of this effect is in preparation.

9.1.3.8 Conclusion

The low calculated values for CH_2 may indicate that the importance in the resonance region is given too low by the calculation. Assuming a higher importance level in this region would also lead to a higher (negative) influence of all resonance absorption effects. This would lower the material worth of ^{235}U (less positive) and of ^{238}U (more negative), and of boron (more negative). A lower value of the material worth of ^{235}U will also result, if a higher σ_c/σ_f value for this material will be selected. For ^{238}U, a lower capture cross section in the resonance region would tend to give better agreement between calculation (based on the SNEAK set) and experiment. A lower capture cross section of ^{238}U would also lead to a higher importance in this region, an effect that was found desirable before. The combination of higher importance and lower capture cross section will still result in a less negative reactivity value for ^{238}U.

9.2 Material Worth Traverses

The material worth as a function of the radial position is given for some materials in fig. 31.

If the experimental and calculated curves are normalized in the core center, the experimental curve shows a flatter distribution across the core. This corresponds to the behavior of rate traverses (see chapter 8.2). This effect may be due to a flatter distribution of the product of flux and adjoint flux throughout the core.

10. Doppler Effect

The temperature dependent reactivity effect of different samples of uranium oxide and of plutonium oxide (see table 20) has been determined in the central zone of assembly 3A-2 using the pneumatic square wave pile oscillator. A drawing of the sample is shown in /1/. The sample and an equivalent dummy were inserted into a fuel element loaded with core material. The temperature was varied from room temperature to slightly above 1000°K. The calculations were done using the method discussed by Fischer in /19/.

10.1 Uranium Oxide Samples

Three samples of .4%, 15%, and 25% enrichment ^{235}U respectively were investigated. The statistical resonance parameters were taken from Schmidt /20/. For ^{238}U resolved resonance parameters are given by Garg et al. /21/ up to 4 keV. They were used in those energy groups of the 26 group set where resolved parameters are available for the whole group interval, which means up to 2.2 keV. For ^{235}U, no significant contribution to the Doppler effect comes from resolved resonances. Expansion effects were found to be negligible. A correction for crystal effects in UO_2 was applied, based on the assumption of weak binding proposed by Lamb /22/ and using the experimental phonon spectrum by Dolling /23/.

The results of experiment and calculation are shown in fig. 32. The deviation between experiment and calculation amounts to 5% or less.

10.2 Plutonium Oxide Samples

Two samples of 154.5 g and 451.7 g plutonium oxide were investigated. The composition of the plutonium is shown in table 20. These measurements were performed with the intention to test the α-value of ^{239}Pu. In contrast to ^{238}U, the Doppler effect of ^{239}Pu is composed of a positive fission contribution and of a negative absorption contribution of similar magnitude, resulting in a rather small net effect of either positive or negative sign. In addition, the expansion effect is greater than for uranium and, finally, the problem of overlap with ^{238}U resonances of the sample environment exists. Therefore, one has to anticipate a greater difference between experiment and calculation.

It should be noted that most earlier experimental results differed greatly from calculated values /24, 25/ and various speculations were made to explain the disagreement.

Two sets of resonance parameters were used for the calculations, first, those given by Schmidt /20/ and, secondly, a set that corresponds to the data determined independently by Pitterle /26/ and Barre /27/ from measurements of σ_t and σ_f ("new data"). Corrections were made for the radial expansion effect. Multilevel effects were estimated using a method following Cook /28/, but were found to be negligible. Kelber and Kier /29, 30/ found that the Doppler changes in the resonance integrals of ^{239}Pu in a mixture with ^{238}U can only be calculated with a large variance, due to overlap effects with ^{238}U resonance. However, it was demonstrated by calculations which were a simplified version of those in /29, 30/ that the variance is much smaller for the sample measurements, where the ^{238}U resonances are stationary, than for the fuel mixture. Thus, the probable error in the calculated Doppler effect due to overlap effects should be at most 20%.

The results of experiment and calculation are shown in fig. 33. The calculations using the "new data" show much better agreement with experimental results than the others. Therefore, the Doppler experiment confirms the "new data". Actually, considering that the magnitude of the calculated net effect is only about 20% of the fission effect, the agreement must be considered satisfactory. It is believed that Doppler measurements with diluted Pu-samples can be interpreted with only minor corrections but without any speculations, if the proper resonance parameters are used.

11. Prompt Neutron Decay Constant

The prompt neutron decay constant has been determined by the Rossi-α method for assemblies 3A-2 and 3A-3. Furthermore, the same constant was determined using the polarity correlation of reactor noise for assembly 3A-2 and using the pulsed source technique for assembly 3A-3.

11.1 Assembly 3A-2

11.1.1 Experiments

Two ^{3}He-counters each were placed in positions 18/17 and 20/21. The resulting reactivity loss had to be compensated by exchanging eight blanket elements with core elements. The ^{3}He-counters were operated in the pulse mode for the Rossi-α experiment and in the current mode for the polarity correlation method.

The Rossi-α method was applied in a manner described by Edelmann /31/ using a new kind of time analyzer. This analyzer was developed for Rossi-α and pulsed source measurements in fast plutonium fuelled reactors to avoid large systematic and statistical errors in the Rossi-α experiment due to deadtime effects in conventional time analyzers. Fig. 34 shows α as a function of reactivity. The value extrapolated for the prompt neutron decay constant amounts to

$$\alpha_c = 1.55 \times 10^4 \text{ sec}^{-1} \pm 1\%.$$

The reactor noise was also analyzed by application of a newly developed two detector cross correlation technique /32/ called polarity correlation in the frequency domain that uses only ac-polarity information from detector signals to measure reactor kinetic parameters. The latter experiment was performed with a reactor power of 200 watts.The signals were stored on magnetic tape and were analyzed using a conventional band filter as well as a dynamic filter. The prompt decay constant was determined as

$$\alpha_c = 1.61 \times 10^4 \text{ sec}^{-1} \pm 3\%.$$

The experimental values for α_c found by two methods independent of each other agree within their respective error limits. Taking the average of the two values results in

$$\alpha_{c,exp} = 1.58 \times 10^4 \text{ sec}^{-1}.$$

11.1.2 Method of Calculation and Discussion of 3A-2 Results

The calculations were based on the original core size of assembly 3A-2, i.e. the additional elements necessary to compensate for the reactivity loss due to the counters were not taken into account. The value of α_c was calculated in two ways: First, the prompt critical neutron life time as well as the effective fraction of delayed neutrons were determined using perturbation theory. Secondly, α was determined by an iterative technique as the eigenvalue of the equation

$$(L + \frac{\alpha}{v}) \phi + P \phi = 0^*$$

in a 26 group diffusion code, using the boundary conditions of the reactor at "delayed critical". To get the prompt production, a value of β_{eff} was selected and the value for ν multiplied by $(1-\beta)$. As the calculations did not yield $k_{eff}=1$ for the critical reactor, the iteration was performed to get the same criticality for the prompt case. For both types of calculations the SNEAK-NORM set was used. The perturbation calculations were also performed using the SNEAK-HET set, and the PMB set also was used for calculations based on the second method. All calculations were done by one-dimensional diffusion theory in cylinder and plate geometry for the perturbation treatment and just in cylinder geometry for the second method. In all cases energy dependent bucklings were used.

Table 21 shows the results of calculating life time and β_{eff} separately by perturbation theory. Two sets of delayed neutron fractions β_i were used to calculate β_{eff}, viz. those for fast and thermal fission for ^{235}U given in /33/. The results of axial calculations are given only. Deviations between axial and radial calculations vary by 0.5% in maximum. The SNEAK-HET set results in a value for α_c by 5% lower than the SNEAK-NORM set, i.e. closer to the experimental value.

---

* L = loss operator; P = prompt production operator; v = neutron velocity

The results of the method using the iteration technique are shown in table 22. The values for the normal SNEAK set agree very well with the ones calculated by the perturbation method. Therefore, it is reasonable to assume the same for the other sets. The PMB-NORM set results in a lower value for α_c than does the SNEAK-NORM set, a heterogeneity corrected version of the PMB set will probably give still a better result. It has to be recalled, on the other hand, that the PMB set gives a less correct k_{eff}. This may have influence on the result by compensation of different errors.

If the relatively higher neutron importance found experimentally around 24 keV is finally confirmed, a use of this value for the perturbation calculations will result in an increase of the calculated neutron life time. This would lead to a better agreement between theory and experiment.

11.2 Assembly 3A-3

Two types of measurements based on the pulsed source and the Rossi-α method were performed immediately after each other. The assembly was left unchanged to permit a direct comparison between the two results. The neutron counters used, however, were not the same, but both sets of counters were in the reactor at the same time.

The two fission chambers used for the pulsed source measurements were placed in positions 21/10 and 22/21. The two fission chambers in blanket positions 11/25 and 13/27 that were normally used as monitors, were also utilized for this experiment. The four ^{3}He-counters used for the Rossi-α method were placed in position 16/21. They were operated in parallel.

The pulsed source used to perform this experiment was the same as was used in assembly 3A-1 /1/, i.e. a 150 keV Cockroft Walton type accelerator with duo-plasmatron ion source. The target was positioned near the core center. The results were evaluated following the area method of Sjöstrand /34/, as far as possible. It was found, that the reactivity scale based on the shim rod calibration by means of the inverse

kinetic program agrees with the one obtained by the Sjöstrand method within the error limits. This had not been the case for assembly 3A-0. Fig. 35 shows α as a function of negative reactivity. From this graph one obtains the value

$$\alpha_c = 1.28 \times 10^4 \text{ sec}^{-1} \pm 1\%.$$

It may be added that an extrapolation of the straight line to $\alpha=0$ leads to $\varrho=1.07\$$.

The Rossi-α decay curves measured for the assembly close to critical can be described by one exponential term. This, however, is not possible for decay curves related to the assembly being more subcritical. Therefore, an evaluation of these results that is based on the point reactor model is inadequate. This is not too surprising, as assembly 3A-3 consists of two core zones of quite different hydrogen content, i.e. of different spectra and different life times. Therefore, this assembly should be treated as a coupled reactor. The respective theoretical treatments /35, 36, 37/ lead to a prompt neutron decay curve that can only be described by a sum of exponential terms. The experimental behavior shown in fig. 36, i.e. a fast decay, followed by a slower one that is followed again by a faster one, has not been observed before. There are no theoretical models in existence to understand this behavior. It is suspected that the change of the spatial source distribution with various degrees of subcriticality and that spectral effects give rise to the problems mentioned. An indication that the source distribution is at least partially responsible for the oscillating character of some of the Rossi-α decay curves has been found by operating a neutron generator during an additional Rossi-α measurement with the assembly being subcritical but under otherwise identical conditions. Thereby the main part of source neutrons was produced near the core center, within the "flooded" core zone. Only one exponential has been found in this experiment. Further experimental investigations should be done to get a better understanding of space and energy dependent reactor kinetics.

Summarizing the results of the Rossi-α experiments led to the conclusion, that the kinetic behavior of assembly 3A-3 is not yet fully understood. Therefore, a comparison of the results of experiment and calculation for the pulsed source experiment is not presented even though the evaluation of the pulsed source experiment did not lead to any difficulties.

12. Reactivity Worth of Control Rods

The assemblies discussed in this paper contained eight shim rods, six safety rods and one fine regulating rod (see fig. 2, 4, 5). The composition of the rods was the same as in assembly 3A-1, with a hydrogen density of 8.17×10^{-24} cm^{-3} in the part of the rods that was filled with core material.

The neutron flux was measured with three ionization chambers at the locations 06/14, 20/31 and 26/06 just outside the reactor blanket in order to obtain more information about space dependent effects. It may be recalled that the results of calibrations with the continous run method in SNEAK-3A-1 had been dependent upon ionization chamber location relative to the control rod location. Deviations from point reactor kinetics are also apparent after a reactivity step through the fact that the reactivity as calculated from the flux output of an ion chamber is not constant after the step. An investigation of this phenomenon has been started after it was found with SNEAK-3A-1 that averaging of the currents of two ionization chambers did not reduce the space dependent effects in all cases markedly. Theoretically it is possible to find a detector location such that point kinetics apply for the calibration of particular rod /38/. In practice this cannot be applied in SNEAK since only a small number of ionization chambers is available and positioning of them close to or inside the core is undesirable because of spectrum perturbations. Corrections for space dependent kinetics based on calculated deviations of flux distributions are considered too cumbersome, assuming that a sufficient approximation can be achieved.

A measure for the deviation from point kinetics is the rate by which the calculated reactivity changes after a step. If, for example, the magnitude of a reactivity step is underestimated the worth calculated with point kinetics will increase with time after the step. In table 23 the reactivity worth obtained by inverse point kinetics just after a rod was driven in and the change of this worth 30 sec later are indicated for three ionization chambers. A "time independent" reactivity worth was obtained by linear interpolation to zero reactivity slope between the results of two ionization chambers. It is hoped that this value is close to the space independent value. This method is demonstrated in fig. 37.

As three experimental points are available to determine the slope of a straight line, one also gets an impression concerning the error of the result. The results are influenced by statistics, as can be seen by comparing two measurements with the same ion chamber. It may also be that the limits are exceeded beyond which linear interpolation is too crude an approximation. The interpolation does not give meaningful results for all data of table 23. Investigations with more experimental material continue.

Another way of improving inverse kinetics rod calibrations lies in moving a rod in small steps and waiting 20 to 30 sec each time instead of driving the rod in continually within 70 sec only. More transients die out in this way and the results of calibrations with two different ion chambers approach each other more closely. This can be seen from the results of stepwise calibration of rods T_1 and T_3 in table 23.

The worth of a shim rod was shown to be rather sensitive to major changes in the reactor core that occured during void and flood experiments: The worth of T_{12} decreased by 16% when going from the core 3A-2 to 3A-3. The interaction with the neighbouring rod T_{14} was also measured: T_{14} was worth 15% more when T_{12} was inserted then when T_{12} was 3/4 driven out and its absorber follower correspondingly driven in.

The worth of individual rods was calculated by one-dimensional diffusion theory in the same way as for assembly 3A-1 /1/. Conversion from absolute units to dollars was made with 1$ = 0.7067%.

13. General Discussion

13.1 Status of Agreement between Experiment and Calculation for Quantities of Interest to a Reactor Designer

13.1.1 Critical Mass

Using the configuration that was actually found critical as a basis for the calculation results in a k_{eff} of 0.988 for the SNEAK set with heterogeneity corrections applied. From the performance of the critical experiment it is known, that a $\frac{\Delta k}{k} \approx -1.2\%$ close to critical corresponds to an underestimation of about 8% in critical mass. For SNEAK assembly 3A-2 this amounts to about 32 kg of ^{235}U. The ABN set results in an overestimation of the critical mass by an amount of similar magnitude.

13.1.2 Reactivity Coefficient of the Coolant

The reactivity effect of either voiding part of the core or doubling the steam density in part of the core is underestimated by the calculation. The error lies between 15% and 20%, the lower figure is related to the void effect.

13.1.3 Breeding Ratio

The initial breeding ratio may be written as

$$\frac{\text{Integrated } ^{238}U \text{ capture rate}}{\text{Integrated } ^{235}U \text{ fission rate}} \times \frac{1}{1 + \bar{\alpha}^{25}}$$

where $\bar{\alpha}^{25}$ means the spatially weighted ratio of capture to fission rate in ^{235}U. A combination of experimental results (reaction rate ratios, material worths, effective source strength of ^{252}Cf) and some calculational corrections to obtain a value for $\bar{\alpha}^{25}$ was found to be of insufficient accuracy. For this reason, a breeding ratio was not

experimentally determined, and, to a lesser extent, because rate traverses were not measured in radial directions. However, the first factor of the expression quoted above was determined for the rates integrated in the axial direction. A higher value of this quantity will lead to a higher breeding ratio. Concerning just this factor, the SNEAK NORM set results in a too optimistic value, while the ABN NORM set results in a too pessimistic one. The deviations from the experimental value are of the same magnitude for both sets, i.e. 4%.

13.1.4 Doppler Effect

The Doppler effect of ^{238}U was calculated within 5% of the experimental value, while for ^{239}Pu the deviation between experiment and calculation was found to be 20%. It must be recalled, however, that the Doppler effect of ^{239}Pu was measured under conditions different from a power reactor as far as ^{238}U resonance overlap is concerned.

13.1.5 Prompt Neutron Decay Constant

This quantity is overestimated by the calculation by an amount of at least 16%.

13.2 Sources of Disagreement between Experiment and Calculation for all Quantities Measured

13.2.1 Identification of Error Sources

The following three main sources that are or may be responsible for the remaining disagreement between experiment and calculation will be covered:

1) Errors in cross section data
2) Incorrect description of heterogeneity effects

3) Incorrect description of rate traverses close to the core-blanket interface and within the blanket.

Errors of the first category are very likely. Concerning the second category, there are many indications, that heterogeneity effects are described quite satisfactorily. The third category, finally, just states a discrepancy that obviously exists.

The integral quantities that have been measured usually are subject to at least two of the possible sources of error mentioned above. Some of them even depend on all three and therefore are not particularly suited to trace errors. This applies to k_{eff}, the normalization integral for perturbation calculations, and the prompt neutron decay constant. In some cases, experimental corrections are possible, for instance for the normalization integral. Similarly, the prompt neutron decay constant could be calculated using the experimental spectrum if this disagrees with the calculated one beyond the error limits.

13.2.2 Cross Section Effects

13.2.2.1 Survey

To obtain a quick survey on the degree of agreement between experiment and calculation the results for those integral data that may be helpful to trace cross section errors are shown in table 24. For the sake of clearness, the data for assembly 3A-2 are shown only.

13.2.2.2 Spectrum and Adjoint Spectrum

While, in general, it is rather difficult to separate discrepancies due to cross section effects from those due to heterogeneity effects, the neutron spectrum and the adjoint spectrum in the energy range from about 10 keV to 1 MeV are practically independent of heterogeneity effects, in particular for the unbunched case. The proton recoil results show that the actual neutron spectrum in the energy range between 50 keV and 800 keV

lies in between the spectra calculated with the SNEAK set or the ABN set, but it is slightly closer to the results based on the SNEAK set. The discrepancy could be solved by the assumption, that inelastic scattering is overestimated by the SNEAK set, but this conclusion is not compulsory. For the energy range between 10 keV and 50 keV, both sets calculate more neutrons than are found by experiment.

The results of the attempt to determine the importance spectrum experimentally lead to an importance by some percent higher than calculated at about 24 keV, if the normalization is made in the high energy region. This behavior indicates a higher ratio of macroscopic fission to absorption cross section for the core mixture than is assumed in the calculation. The deviations can lie in the energy range around 20 keV or below. In the latter case, the discrepancy has to be interpreted as the "upscattered tail" of a larger discrepancy at lower energies. An increased importance around 20 keV or below will result in higher material worths for scatterers and in a higher neutron life time. Both changes would improve the agreement between calculation and experiment

The neutron spectrum measured by the sandwich method in the energy range below 3 keV is strongly influenced by heterogeneity effects. In this energy range the results of experiment and of calculations based on the SNEAK HET set agree within the experimental error limits. Heterogeneity corrected ABN cross sections were not used.

13.2.2.3 Reaction Rate Ratios

It is recalled, that the discrepancies between experiment and calculation for reaction rate ratios do not favor the use of either the SNEAK set or the ABN set, they are of the same order in both cases.

Lack of agreement between a carefully evaluated experiment and a calculation of a reaction rate ratio can be due to a wrong spectrum used for the calculation or to errors in the cross sections of one or both reaction rates concerned, or, finally, to a combination of these effects. The error in spectrum may, of course, also be due to cross section errors of one of the materials whose rates are part of the spectral index.

However, as the spectrum can be measured over quite a large energy range, it is practical to separate this effect.

The ratio of the ^{238}U capture rate to the ^{235}U fission rate is not very sensitive to a revision of the spectrum as made probable by the proton recoil measurements because both rates are influenced quite similarly. Therefore, a revision of cross sections should be considered, possibly a reduction of the ^{238}U capture cross section. Admittedly, this picture can change, if the relative position of the two parts of the experimental spectrum (sandwich method and proton recoil method) is found to deviate from the one calculated.

The central ratio of the fission rates of ^{238}U to ^{235}U shows a deviation of about 13% between experiment and calculation. The fission rate of ^{238}U is not influenced by the discrepancies found between the experimental and the calculated spectrum. As the distribution of the contributions of different energy groups to the ^{235}U fission rate shows a rather flat behavior in the energy range between 1 keV and 1 MeV, it is very unlikely that a discrepancy in spectra in this region can give rise to a major change of the value of the fission rate. Therefore, also in this case a revision of group cross sections appears to be appropriate.

13.2.2.4 Rate Fine Structure

Calculations of rate fine structure were performed by means of the SNEAK set only. While the experimentally found local fine structure of the fission and the capture rates of ^{238}U is quite well described by the calculations, there are discrepancies for the fission rate of ^{235}U. This, again,may be a consequence of cross section errors. It is recalled, however, that the fine structure of the ^{235}U fission rate is composed of contributions of opposite sign and, therefore, is more sensitive to cross section errors than the others.

13.2.2.5 Material Worths

The experimental values for the material worths of ^{235}U and ^{238}U are in favor of using the ABN set, the few values for Pu do not allow a decision between the two sets. It may be recalled, however, that material worth measurements were not yet done under conditions as easily interpretable as is the case for some of the reaction rate ratios. Furthermore, lack of agreement between experimental and calculated materials worths can be due to either one or to a combination of the following effects: Errors in normalization integral, errors in flux spectrum used, errors in adjoint spectrum used, errors in cross sections of materials concerned. There are experimental indications, that the first three sources of errors are present, the presence of the last one is rather probable. There is no experimental information available concerning the importance spectrum below 20 keV, i.e. in a range that will give rise to roughly half of the capture contribution. For all these reasons, the discussion of experimental material worth measurements is still in a more speculative state than that of reaction rate ratios, for example.

13.2.2.6 Doppler Effect

The Doppler experiments showed that the resonance parameters of ^{238}U are known well enough to allow a good theoretical estimate of the Doppler effect. For ^{239}Pu, the experiments are clearly in favor of the "new data", i.e. those given in /26/ and /27/.

13.2.3 Heterogeneity Effects

The reactivity changes due to bunching are described quite satisfactorily by calculations using the SNEAK set. This is so in spite of the fact that the main reaction rate ratios cannot be calculated very well, and that the same applies to the fine structure of the fission rate of ^{235}U. It is assumed that the bunching experiments are not too

sensitive to errors in absolute cross sections but depend primarily on the changes of cross sections averaged over the fuel zone due to bunching. These changes then are well described by the ZERA program.

The reasons for the discrepancies, particularly for assembly 3A-3, concerning the flux fine structure measured by gold and copper sandwiches are not yet known. These effects will be further investigated in the assemblies to follow.

13.2.4 Behavior of Rate Traverses Close to the Core-Blanket Interface and in the Blanket

It was already observed at assembly 3A-1 that experiment and calculation disagree markedly in this aspect, and the results of the respective chamber measurements are very similar for assembly 3A-2. Foil measurements that were performed at assembly 3A-2 only, lead to results different from the calculated ones as well as from the chamber results. While the experimental discrepancy is probably due to streaming effects, the disagreement between the foil experiments, that are considered more reliable, and the calculations is not yet understood.

13.3. Conclusion

The experimental results as a whole do neither favor the use of the SNEAK set nor of the ABN set. Some corrections of basic cross section data appear still to be necessary to both sets to achieve better agreement with experimental results. Concerning ^{239}Pu, the cross section data based on evaluations by Pitterle and Ribon have been shown to improve the agreement between experiment and calculation for the Doppler effect. Heterogeneity effects are quite well understood as far as their reactivity influence is concerned. The remaining discrepancies in rate and flux fine structure may in part be due to errors in cross sections, but they should be further studied. The behavior of rate traverses at the blanket interface and within the blanket is not yet understood.

Acknowledgement

The authors gratefully acknowledge the continuous support by the operation staff of the SNEAK reactor during the performance of their experiments.

We are also indebted to Dr. H. Küsters, Dr. J.J. Schmidt, and Dr. D. Stegemann for helpful discussions.

References:

/1/ Stegemann, D. et al., KFK-627 (1967)

/2/ Wintzer, D., KFK-633 (1967)

/3/ Huschke, H. et al., KFK-770 (1968)

/4/ Pönitz, W.P. et al., KFK-635 (1967)

/5/ Abagjan,L.P. et al., KFK-tr-144
German Translation of "Group Constants of Fast and Intermediate Neutrons for the Calculation of Nuclear Reactors," States Committee for the Use of Atomic Energy in the USSR

/6/ Engelmann, P, Raberain, A.M., Wintzer, D., KFK-776 (1968)

/7/ Benjamin, P.W. et al., AWRE NR 2/64 (1964)

/8/ Bennett, E.F., Rev. Sci. Instr. 35, 1153 (1962)

/9/ Connolly, T.J., de Kruijf, F., Schmidt, J.J., KFK-718 (1968)

/10/ Meadows, J.W., Phys. Rev. 157, 1076 (1967)

/11/ Thomson, M., Taylor, J.M., Nucl. Inst. Meth. 37, 307 (1965)

/12/ Geiger, K.W., Hargrove, C.K., Nucl. Phys. 53, 204 (1964)

/13/ Geiger, K.W., Jarvis, C.J.D., Can. Journ. of Phys. 40, 33 (1962)

/14/ Szilvasi, A., J. Nucl. Energy 11, 132 (1960)

/15/ Bennett, E.F., ANL-7110, 337 (1965)

/16/ Schmitt, H.W., Nucl. Phys. 29, 220 (1960)

/17/ Seufert, H., Stegemann, D., Nucl. Sci. and Eng. 28, 227 (1967)

/18/ Böhme, R., Seufert, H., KFK-811 (1968)

/19/ Fischer, E.A., KFK-473 (1966)

/20/ Schmidt, J.J. KFK-120 (1966)

/21/ Garg, J.B. et al., Phys. Rev. 134, B 985 (1965)

/22/ Lamb, W.E., Phys. Rev. 55, 190 (1939)

/23/ Dolling, G. et al., Can. Journ. of Phys. 43, 1397 (1965)

/24/ Fischer, G.J. et al., Nucl. Sci. and Eng. 25, 37 (1966)

/25/ Greebler,P. et al., ANL-7320, 66 (1966)

/26/ Pitterle, T.A. et al., Conf. on Neutron Cross Section Technology, Washington 1968

/27/ Barre, J.Y. et al., Conf. on Neutron Cross Section Technology, Washington 1968

/28/ Cook, J.L., Austr. Journ. of Phys. 20, 67 (1967)

/29/ Kelber, C.N., Kier, P.H., Nucl. Sci. and Eng. 24, 389 (1966)

/30/ Kelber, C.N., Kier, P.H., Nucl. Sci. and Eng. 26, 67 (1968)

/31/ Edelmann, M., Karlsruhe External Report INR-4/68-15, 1968

/32/ Seifritz, W., to be published

/33/ Keepin, G., Physics of Nuclear Kinetics, Addison Wesley (1965)

/34/ Sjöstrand, N.G., Arkiv Fysik 11 (1956)

/35/ Cohn, C.E., Nucl. Sci. and Eng. 13, 12 (1962)

/36/ Kistner, G., Nukleonik 7, 106 (1965)

/37/ Borgwaldt, H., Santiz, D., Nukleonik 5, 239 (1963)

/38/ Köhler, B., Kernenergie 11, 331 (1967)

Table 1: Characteristics of Uranium-Hydrogen Assemblies Investigated in the SNEAK-3A Series

Assembly No.	Corresponding central zone steam density (g H_2O/cm^3) in the coolant volume (35%)	Critical data *)		^{235}U fissions below 10 keV in the central core zone (%)
		mass ^{235}U (kg) in core	core volume (l)	
3A-0	0		**)	8
3A-1	0.0317	524.5 ±1.0	664.3 ±1.0	24
3A-2	0.0757	400.3 ±0.9	505.3 ±1.4	38
3A-3	0.1514		**)	50

*) The critical data are given for an idealized cylindrical core.

**) Critical data were not determined for assemblies having two core zones of different hydrogen density.

Table 2: Atom Densities (in 10^{20} cm^{-3}) of SNEAK Assembly 3A-2 Used for Homogeneous Calculations

	Al	C	Co[1]	Cr	Fe	H	Mg[2]	Mn[3]	Ni	O	Si	Ti	^{235}U	^{238}U	Mo+Nb
Core Zone 1	129.10	9.32	0.19	34.53	121.85	17.92	0.64	1.94	18.54	145.29	1.88	0.40	20.31	81.04	0.39
Core Zone 2	129.36	9.08	0.18	34.36	121.33	17.45	0.64	1.96	18.27	145.67	1.86	0.39	20.25	81.21	0.39
Blanket	-	0.14	-	11.08	39.55	-	-	0.87	9.84	-	0.46	-	1.625	399.414	0.19

[1] Co was added to Fe for the calculation

[2] Mg was added to Al " " "

[3] Mn was added to Cr " " "

Table 3: Atom Densities (in 10^{20} cm^{-3}) for the Core Zones of SNEAK Assembly 3A-2 Used for Heterogeneity Calculations (Thickness of all platelets: 3.14mm)

	Material / Platelet	Al(+Mg)	C	Cr(+Mn)	Fe(+Co)	H	Mo	Ni	O	Si	Ti	^{238}U	^{235}U
Core Zone 1	U 20%	0	0	1.17-3	3.892-3	0	0	1.272-3	0	0	0	3.2416-2	8.124-3
	Al_2O_3	3.8766-2	0	1.17-3	3.892-3	0	0	5.67-4	5.8116-2	0	0	0	0
	$SS+CH_2$	0	3.731-3	1.1005-2	3.7165-2	7.168-3	1.58-4	5.011-3	0	6.45-4	1.63-4	0	0
	Al(25%)	1.3121-2	0	1.217-3	3.892-3	0	0	5.67-4	0	1.08-4	0	0	0
Core Zone 2	U 35%	0	0	1.155-3	3.809-3	0	0	1.243-3	0	0	0	2.592-2	1.434-2
	U_x *)	0	0	1.155-3	3.809-3	0	0	1.243-3	0	0	0	3.905-2	1.859-3
	Al_2O_3	3.869-2	0	1.155-3	3.809-3	0	0	5.37-4	5.8268-2	0	0	0	0
	$SS+CH_2$	0	3.632-3	1.100-2	3.726-2	6.980-3	1.58-4	4.985-3	0	6.337-4	1.557-4	0	0
	Al(25%)	1.332-2	0	1.202-3	3.809-3	0	0	5.37-4	0	1.09-4	0	0	0

*) The actual unit cell of core zone 2 (see fig. 3) was formed of 36 platelets. This rather large cell was necessary, because the desired average ^{235}U enrichment of 20% had to be achieved by using 35% enriched and natural uranium platelets. For the calculations the following simplified cell structure was used

$$/SS+CH_2/Al_2O_3/U35\%/Al(25\%)/SS+CH_2/Al_2O_3/U_x/Al(25\%)/.$$

The amount of ^{235}U and ^{238}U in the platelet U_x was adjusted to result in the same homogenized densities in core zone 2 for the actual and the simplified unit cell.

Table 4: k_{eff} Calculated for the Actually Critical Configuration of SNEAK Assembly 3A-2

Cross section set	SNEAK set	ABN set	PMB set
k_{eff} (1-dim. 26 groups, homog. calculation)	0.9835	1.006	0.9795
heterogeneity correction	+0.0024		
Correction for 2-dim. calculation	+0.0020		
k_{eff} (corrections applied)	0.9879	(1.0102)*)	(0.9839)*)

*) These values result in case the corrections, calculated for the SNEAK set only, are applied.

Table 5: Comparison of Experiment and Calculation for the Void Experiment in SNEAK Assembly 3A-1

Step	Negative Reactivity Effect Δk/k (%)		Calculation / Experiment
	Experiment	Calculation SNEAK HET	SNEAK HET
1a	0.164	0.140	0.85
1b	0.304	0.267	0.87
1c	0.410	0.365	0.89
1d	0.459	0.406	0.89
2	0.935	0.825	0.88
3	1.079	0.947	0.88
4	1.214	1.051	0.86
5 total core	3.18 (extrapolated)	2.79	0.88

Table 6: Composition of the Breeder Blanket

Material	Atom densities (10^{24} cm^{-3})	
	normal	voided
C	9.5047-4	3.10796-5
Cr	2.54688-3	2.54688-3
Fe	8.74029-3	8.74029-3
H	1.8388-3	-
Ni	1.2768-3	1.2768-3
O	0.0200735	0.0200735
Si	1.54126-4	1.54126-4
Ti	6.51-5	6.51-5
^{235}U	4.05685-5	4.05685-5
^{238}U	9.97391-3	9.97391-3

Table 7: Comparison of Experiment and Calculation for the Void Experiment in SNEAK Assembly 3A-2

SNEAK blanket: metallic uranium (see table 2)
Breeder blanket: uranium oxide (see table 6)

Step	Blanket	Height of voided zone	Negative Reactivity Effect Δk/k (%)		Calculation / Experiment
			Experiment	Calculation SNEAK HET	
1	Breeder	25% of core zone	0.177	0.154	0.87
2	"	core zone	0.506	0.427	0.84
3	"	core and axial blanket	0.497	0.420	0.84
4	SNEAK	25% of core zone	0.177	0.147	0.83
5	"	core zone	0.498	0.413	0.83

Table 8 Comparison of Experiment and Calculation for the Flooding Experiment in SNEAK Assembly 3A-2

Step	Positive Reactivity Effect Δk/k (%)		Calculation / Experiment
	Experiment	Calculation SNEAK HET	
1a	0.188	0.153	0.81
1b	0.348	0.283	0.81
1c	0.460	0.376	0.82
1d	0.517	0.418	0.81
2a+b	1.18	0.92	0.78
2c+d+e	1.97	1.51	0.77
3a+b+c+d	2.32	1.76	0.76
4 total core	5.9 (extrapolated)	4.62	0.78

Table 9: Characteristic Data of Resonance Activation Foils

Material	Energy of main resonance *)	Group No	Material used	Thickness (μ)	Z **)	Characteristic Factors ***) SNEAK-3A-0 R(%)	SNEAK-3A-0 F(%)	SNEAK-3A-1 R(%)	SNEAK-3A-1 F(%)	SNEAK-3A-2 R(%)	SNEAK-3A-2 F(%)	SNEAK-3A-3 R(%)	SNEAK-3A-3 F(%)
Na-23	2850 eV	13	NaF	500	1	2.6	85.0	2.6	94.9	3.2	97.0	2.4	97.9
Cu-63	577 eV	13	metal	100	32	1.3	36.7	3.3	74.5	5.7	81.9	5.3	86.5
Mo-98	467 eV	15	metal	200	10	0.8	26.8	2.1	60.5	4.6	67.0	4.2	70.8
Mn-55	337 eV	16	metal +12% Ni	50	7					5.2	70.6	4.8	75.4
Cd-114	120 eV (1107 eV)	17	metal	500	6	0.25	5.6	0.9	17.4	2.1	27.7	4.2	34.6
Br-81	101 eV (136 eV)	17	KBr	500	3	0.8	2.6	4.5	20.9	8.3	27.6	10.5	33.1
La-139	72.4 eV	18	metal	250	1	0.5	1.0	2.8	19.1	5.4	27.6	8.9	34.8
W-186	18.8 eV (218 eV)	20	metal	25	27	0.2	12.9	4.5	80.6	11.8	89.3	17.3	93.8
Sm-152	8.04 eV	21	metal	75	1					20.1	67.9	27.9	75.1
Au-197	4.91 eV (293 eV)	21	metal	25	62	0.15	4.2	2.4	52.0	6.7	68.7	11.9	79.8
In-115	1.46 eV (83.5 eV)	23	metal (50%Pb)	50	11	6.2	0.2	3.6	89.3	9.2	94.3	15.0	96.4

*) Values in brackets refer to assembly 3A-0 only.

**) Number of resolved resonances considered

***) R Experimental difference between the activities of the outer and inner foil of the sandwich divided by one half of the sum-acitivity

F calculated ratio of activity due to the main resonance to activity due to all resonances considered

All separated resonances known are considered up to 100 keV /9/. Unresolved resonances are considered for all materials.

Table 10: Comparison of Experimental and Calculated Effective Source Strengths for SNEAK Assembly 3A-2. All Values are Normalized to ^{252}Cf.

Source	Experiment	Calculation	
		SNEAK NORM	ABN NORM
^{252}Cf	1.862 ±1%	1.862	1.862
Am/Be	2.01 ±2%	2.016	2.006
Am/B	1.89 ±2%	1.905	1.90
Am/F	1.79 ±1.5%	1.794	1.795
Am/B10	1.82 ±3%	1.834	1.832
Am/Li	1.78 ±4%	1.749	1.765
Sb/Be	1.97 ±1.5%	1.864	1.90

Table 11: Reaction Rate Ratios at the Center of Assembly 3A-2

Method of Measurem.	Reaction Rate Ratio	Experimental Value	Calculation				Calculation/Experiment			
			SNEAK				SNEAK			
			HET	NORM	PMB NORM	ABN NORM	HET	NORM	PMB NORM	ABN NORM
foils	$\frac{^{238}U \text{ fission}}{^{235}U \text{ fission}}$	$3.38 \times 10^{-2} \pm 3\%$	2.93×10^{-2}	2.94×10^{-2}	2.95×10^{-2}	3.01×10^{-2}	0.87	0.87	0.87	0.89
	$\frac{^{238}U \text{ capture}}{^{235}U \text{ fission}}$	$0.130 \pm 3\%$	0.1384	0.1373	0.1361	0.1223	1.06	1.05	1.045	0.94
ionization chambers	$\frac{^{238}U \text{ fission}}{^{235}U \text{ fission}}$	$3.13 \times 10^{-2} \pm 3\%$	2.93×10^{-2}	2.94×10^{-2}	2.95×10^{-2}	3.01×10^{-2}	0.94	0.94	0.945	0.96
	$\frac{^{233}U \text{ fission}}{^{235}U \text{ fission}}$	$1.48 \pm 3\%$	1.560	1.553	1.610	1.437	1.05	1.05	1.09	0.97
	$\frac{^{239}Pu \text{ fission}}{^{235}U \text{ fission}}$	$1.007 \pm 3\%$	0.961	0.953	0.987	0.993	0.955	0.945	0.98	0.985
	$\frac{^{232}Th \text{ fission}}{^{238}U \text{ fission}}$	$0.209 \pm 6\%$	0.1982	0.1982	0.1981	0.1944	0.95	0.95	0.95	0.93

Table 12: **Reaction Rate Ratios at the Center of Assembly 3A-0**

Ratio	Experiment	Calculation SNEAK NORM	Calculation / Experiment
$\frac{^{238}U \text{ fission}}{^{235}U \text{ fission}}$	$3.49 \times 10^{-2} \pm 3\%$	3.247×10^{-2}	0.93
$\frac{^{233}U \text{ fission}}{^{235}U \text{ fission}}$	$1.45 \pm 3\%$	1.604	1.11
$\frac{^{239}Pu \text{ fission}}{^{235}U \text{ fission}}$	$1.03 \pm 3\%$	0.989	0.96
$\frac{^{232}Th \text{ fission}}{^{238}U \text{ fission}}$	$0.203 \pm 6\%$	0.197	0.97

Table 13: Reaction Rate Ratios at the Center of Assembly 3A-3

Ratio	Experiment	Calculation SNEAK NORM	Calculation / Experiment
$\frac{^{238}U \text{ fission}}{^{235}U \text{ fission}}$	2.95×10^{-2} $\pm 3\%$	2.640×10^{-2}	0.89
$\frac{^{233}U \text{ fission}}{^{235}U \text{ fission}}$	1.61 $\pm 3\%$	1.597	0.99
$\frac{^{239}Pu \text{ fission}}{^{235}U \text{ fission}}$	1.11 $\pm 3\%$	1.011	0.91

Table 14 Comparison of Calculated and Experimental Bucklings Associated with Foil Activation Traverses Along the Central Core Axis. The Calculations are Based on the Heterogeneous SNEAK SET and Diffusion Theory

Rate	Buckling $10^4 \times B^2$ (cm^{-2})		$\frac{B^2_{cal}}{B^2_{exp}}$
	experimental	calculated	
^{238}U fission	8.92 $\pm$0.03	9.16	1.03
^{238}U capture	7.87 $\pm$0.02	8.28	1.05
^{235}U fission	8.03 $\pm$0.03	8.40	1.05

Table 15: Reaction Rates Integrated in Direction of the Zylinder Axis

Integrated Rate (sec^{-1} cm^{-2})	Experiment	Calculation / Experiment *)		
		SNEAK NORM	PMB NORM	ABN NORM
$^{28}N \int_{core} \langle \sigma_c^{28} \varphi \rangle dz$	$(5.23 \pm 0.10) \times 10^8$	1.057	1.048	0.940
$^{28}N \int_{blanket} \langle \sigma_c^{28} \varphi \rangle dz$	$(2.56 \pm 0.06) \times 10^8$	0.999	1.003	0.985
$^{25}N \int_{core} \langle \sigma_f^{25} \varphi \rangle dz$	$(1.006 \pm 0.023) \times 10^9$	———	1.000 **)	———
$^{25}N \int_{blanket} \langle \sigma_f^{25} \varphi \rangle dz$	$(7.90 \pm 0.02) \times 10^6$	1.018	1.022	1.088
RATIO $\dfrac{^{28}N \int_{core+blanket} \langle \sigma_c^{28} \varphi \rangle dz}{^{25}N \int_{core+blanket} \langle \sigma_f^{25} \varphi \rangle dz}$	0.77 ± 0.03	1.039	1.034	0.957

*) diffusion theory

**) used for normalization

Table 16: Experimental Bucklings for Vertical Fission Chambers Traverses at Different Distances from the Center Axis of SNEAK Assembly 3A-2

Horizontal Position	Distances from center axis (cm)	$10^4 \times B^2$ (cm^{-2})			
		^{235}U	^{238}U	^{239}Pu	^{237}Np
19/19	0	7.57	-	7.60	8.19
19/16	16.32	7.60	-	7.58	8.11
22/18	17.21	7.98	8.33	7.89	-
19/14	27.20	8.08	8.52	8.06	-
19/12	38.08	8.15	8.53	8.22	-
19/10	48.96	8.24	8.51	8.25	-
19/8	59.84	8.26	-	8.25	-

Table 17: Composition of Uranium and Plutonium Samples. The Reactivity Contributions of the "Other Components" and of Uranium for the 31.8 g Plutonium Sample were Subtracted Using Experimental Data to Give the Results of Table 18.

Sample as characterized in table 18		Weight refers to	Fuel composition (%)				Component other than fuel	Weight ratio: $\frac{\text{other component}}{\text{fuel}}$
Material	Weight (g)		^{235}U	^{238}U	$^{239}Pu+^{241}Pu$ *)	^{240}Pu		
^{235}U	all weights	^{235}U content	93.4	6.6	-	-	no	-
^{238}U	all weights	total uranium	0.4	99.6	-	-	no	-
Pu	2.5	total plutonium	-	-	91.6	8.4	Al	78
	5.0	total plutonium	-	-	91.6	8.4	Al	63
	31.8	total plutonium	0.5	72.9	24.4	2.2	O Stainless Steel	11.7 9.9

*) $\frac{\text{Amount } ^{241}Pu}{\text{Amount } ^{239}Pu} < 1\%$

Table 18: Experimental Central Material Worths ($/kg x 10^3)

Material	Weight (g)	Assembly						
		3A-0		3A-1		3A-2		3A-3
		Core Mat.	Void	Core Mat.	Void	Core Mat.	Void	Void
^{235}U	3.4	304±15		334±6	333±7			440±10
	17.8	302±2	287±3			411±2	353±1	450±4
^{238}U	62	-19.5±0.8	-21±2	-22.5±0.3	-24.1±0.4		-32±2	-38.0±0.5
	262	-18.1±0.1				-26.0±0.5	-29.8±0.3	-33.8±0.1
	998	-					-27.1±0.1	-29.8±0.1
Pu	2.5							607±6
	5.0	465±6						
	31.8	476±8	464±8	433±5	416±5	532±21	506±5	
^{10}B	0.3	-6940±90				17300±600		26000±100
	1.0	-6590±50	-6640±60			14680±150	14850±150	
	2.9		-6400±20	-8390±10	-8550±7	12800±50		18000±100
Ta	53	-100±1			-147±8	-223±10	-228±3	-342±1
Mo	34	-40±1	-40±2		-48±0.7			-93±1
Ni	114	-15.6±0.7			-14.2±0.6		-22±1	
Fe	128	-7.2±0.3			-8.7±0.5	-12 ±1	-12±1	-11.7±.5
Cr	92.6	-9.1±0.3			-7.6±0.3			
CH_2	2.5	2390±20	2370±20	2350±8	2340±7	2520±10		2460±10
	3.6						2310±40	
C	12							74±6
	36	35±2						
	48			55.7±0.6	55.5±1.0	72.4± .4	61±4	
	97							74.2±0.5
O*)	114	15±1					25.6±2	24.9±0.04
Al	160		-5.66±0.05	-2.3±0.2	-2.1±0.2	-07±0.4	-1.2±0.4	+0.9±0.3

*) in Al_2O_3

Table 19: Ratio of Calculated to Experimental Central Material Worths

Material	Weight (g)	Assembly									
		3A-0		3A-1				3A-2		3A-3	
		SNEAK NORM		SNEAK NORM		ABN NORM		SNEAK NORM		SNEAK NORM	ABN NORM
		C.M.	Void	C.M.	Void	C.M.	Void	C.M.	Void	Void	Void
^{235}U	3.4	1.12		1.15	1.15	1.09	1.09			1.20	1.11
	17.8	1.11	1.17					1.08	1.25	1.18	1.09
^{238}U	62	1.29	1.14	1.27	1.20	0.90	0.96		1.10	1.16	0.90
	262	1.33						1.35	1.18	1.28	0.99
	998								1.30	1.45	1.13
Pu	2.5									0.92	1.02
	5.0	1.02									
	31.8	1.00	1.02	1.05	1.10	1.07	1.12	1.07	1.13		
^{10}B	0.3	0.96						1.02		1.28	1.08
	1.0	1.01	1.01					1.20	1.20		
	2.9		1.04	1.24	1.26	1.01	1.03	1.38		1.86	1.57
Ta	53					1.33	1.33				
Mo	34	1.06	1.06		1.28		1.17			1.70	
Ni	114	1.30			1.73						
Fe	128	1.58			1.47		1.05	1.50	1.50	2.00	
Cr	92.6	1.16			1.39		1.58				
CH_2	2.5	0.63	0.63	0.66	0.66	0.62	0.62	0.72	0.79	0.68	0.73
	3.6										
C	12			0.25	0.25	0.60	0.60	0.40	0.45	0.33	0.58
	36	0.06									
	48										
	97									0.33	
O	114	0.11							0.65	0.70	0.80
Al	160		1.82	4.30	4.70	1.95	2.05	13.	7.5	-10.	-4.

Table 20: Data of Doppler Samples

Material	Enrichment ^{235}U (%)	Length (cm)	Diameter (cm)	Weight (g) U	Weight (g) UO_2
UO_2	0.4	9.0	3.5	754	854
UO_2	15.0	9.0	3.5	754	854
UO_2	25.0	9.0	3.5	754	854
	^{240}Pu content (%)			Weight (g) PuO_2	Weight (g) Al_2O_3
PuO_2	8.2	15.0	3.5	154.5	463.5
PuO_2	8.2	15.0	3.5	451.7	360.5

Table 21: Comparison of Experimental and Calculated Values (Perturbation Method, Cylinder Geometry) for the Prompt Neutron Decay Constant α_c of SNEAK Assembly 3A-2

l prompt neutron lifetime

ß effective delayed neutron fraction

Indices: t calculation based on thermal neutron data

f calculation based on fission neutron data

	Calculation		Experiment
	SNEAK HET	SNEAK NORM	
$10^7 \times l$ (sec)	3.835	3.659	
$10^3 \times ß_t$	7.12	7.14	
$10^3 \times ß_f$	7.05	7.07	
$10^{-4} \times \alpha_{c,f}$ (sec^{-1})	1.84	1.93	
$10^{-4} \times \alpha_c^{exp}$ (sec^{-1})	-	-	1.58
$\alpha_c^{calc}/\alpha_c^{exp}$	1.165	1.23	-

Table 22: Comparison of Experimental and Calculated Values (α-Iteration Method) for the Prompt Neutron Decay Constant α_c in SNEAK Assembly 3A-2

$\beta_{eff} = 7.1 \times 10^{-3}$ was used for all sets to obtain α_c.

	SNEAK NORM	PMB NORM	Experiment
k_{eff}	0.9835	0.9795	1.000
$10^{-4}\,\alpha_c$ (sec^{-1})	1.95	1.87	1.58
$\alpha_c^{calc}/\alpha_c^{exp}$	1.235	1.18	-

Table 23: Reactivity Worth of Control Rods in Assembly 3A-2

Rod No.	Position (x/y)	Worth obtained by inverse kinetics with ion chambers at indicated locations (x/y)						Space independent worth (¢) inter-polated	Calc. 1-dim. diff. SNEAK NORM (¢)	Comments
		06/14		26/06		20/31				
		reactivity (¢)	change after 30 sec	reactivity (¢)	change after 30 sec	reactivity (¢)	change after 30 sec			
T_{01}	17/23	103.44	+0.32	100.09	+0.89			105.31±.05		
				100.26	+0.92	108.76	-0.62		92	
				102.76	+0.64	107.27	-0.75	104.96		calibr.in steps
T_{03}	23/17	104.04	+0.80	110.07	+0.34					
				110.00	+0.02	103.88	+0.39			
				109.22	-0.46	103.73	+0.24		92	
				107.57	-0.49	104.34	+0.44	106.02		calibr.in steps
T_{09}	14/20	92.79	-0.21	86.00	+0.73					
				85.74	+0.56	87.40	+0.19	89.83±.9	83	

Table 24: Survey of Deviations Between Experiment and Calculation That May Be Due to Errors in Cross Sections for SNEAK Assembly 3A-2

Quantity	Experimental Error	Typical Value for $\frac{\text{Calculation-Experiment}}{\text{Experiment}}$		Comments
		SNEAK set	ABN set	
k_{eff}	$\pm 0.035\%$ [1]	-1%	+1%	2-dim. diffusion calculation with heterogeneity correction using the experimentally determined critical dimensions
Local Finestructure of Reaction Rates within the Fuel Platelet				
^{235}U fission rate	see fig. 16	deviation s. fig.16		Foil activation within fuel platelet. Calculations with ZERA code
^{238}U fission rate		no deviation within exp. error limits		
^{238}U capture rate				
Spectrum [2]	40keV - 1.1MeV : $\pm 2\%$ - $\pm 4\%$	0 to -15% [3]	+10% to -10% [3]	proton recoil counters
	10keV - 40 keV : $\pm 15\%$	+35% to +65% [3]	+5% to +65% [3]	proton recoil counters, exp. error due to difficulties in γ-n discrimination is probably larger than stated.
	5 eV - 3 keV : $\pm 10\%$ - $\pm 25\%$	no deviation within exp. error limits	4)	sandwich foil activation, calculation uses heterogeneity corrected cross sections
Importancespectrum [2]	> 24 keV : $\pm 1\%$ - $\pm 4\%$	no deviation within exp. error limits		Source spectra taken from literature. No heterogeneity corrections applied.
	24 keV : $\pm 1.5\%$	-5.5%	-3.5%	
Reaction Rate Ratios [2]				
$\sigma_f(^{238}U)/\sigma_f(^{235}U)$	$\pm 3\%$	-13%	-11%	Foil activation within fuel platelet. SNEAK set: calculation with ZERA code. ABN set: homogeneous calculation. Judging from the equivalent SNEAK set results, this does not introduce an error of more than 1%.
$\sigma_c(^{238}U)/\sigma_f(^{235}U)$	$\pm 3\%$	+6%	-6%	
Materialworths [2]				
^{235}U	$\pm 0.5\%$	+15%	(+10%)	Calculations were done by perturbation theory. This does not describe the actual situation. No heterogeneity corrections are applied. ABN set data are interpolated from 3A-1 and 3A-3 results
^{238}U	$\pm 1\%$	+15%	(-5%)	
CH_2	$\pm 0.5\%$	-25%	(-33%)	
Doppler Effect [2]		calculated with special cross sections		
^{238}U	$\pm 3\%$	$\pm 5\%$		Heterogeneity effects are taken into account. "New data" are used for ^{239}Pu calculations. These are based on data evaluations by Pitterle and Barre
^{239}Pu	$\pm 5\%$	-20%		
Prompt Neutron Lifetime	$\pm 1\%$ - $\pm 2\%$	-16%	(-30%)	Heterogeneity corrected cross sections are used for the SNEAK set data. The ABN data were interpolated from 3A-1 and 3A-3 calculations, their heterogeneity correction is estimated on the basis of SNEAK set results.

1) Calculated from error in critical mass (0.23%) and from $\frac{\Delta m}{m} / \frac{\Delta k}{k} = 6.63$ that was found experimentally.

2) Values shown are for core center

3) The experimental and the theoretical spectrum were normalized to equal area below the curve $\varphi(u)$ versus u from 10 keV to 1.1 MeV.

4) Heterogeneity effects are very important in this energy range, but ABN set cross sections corrected for heterogeneity effects were not established.

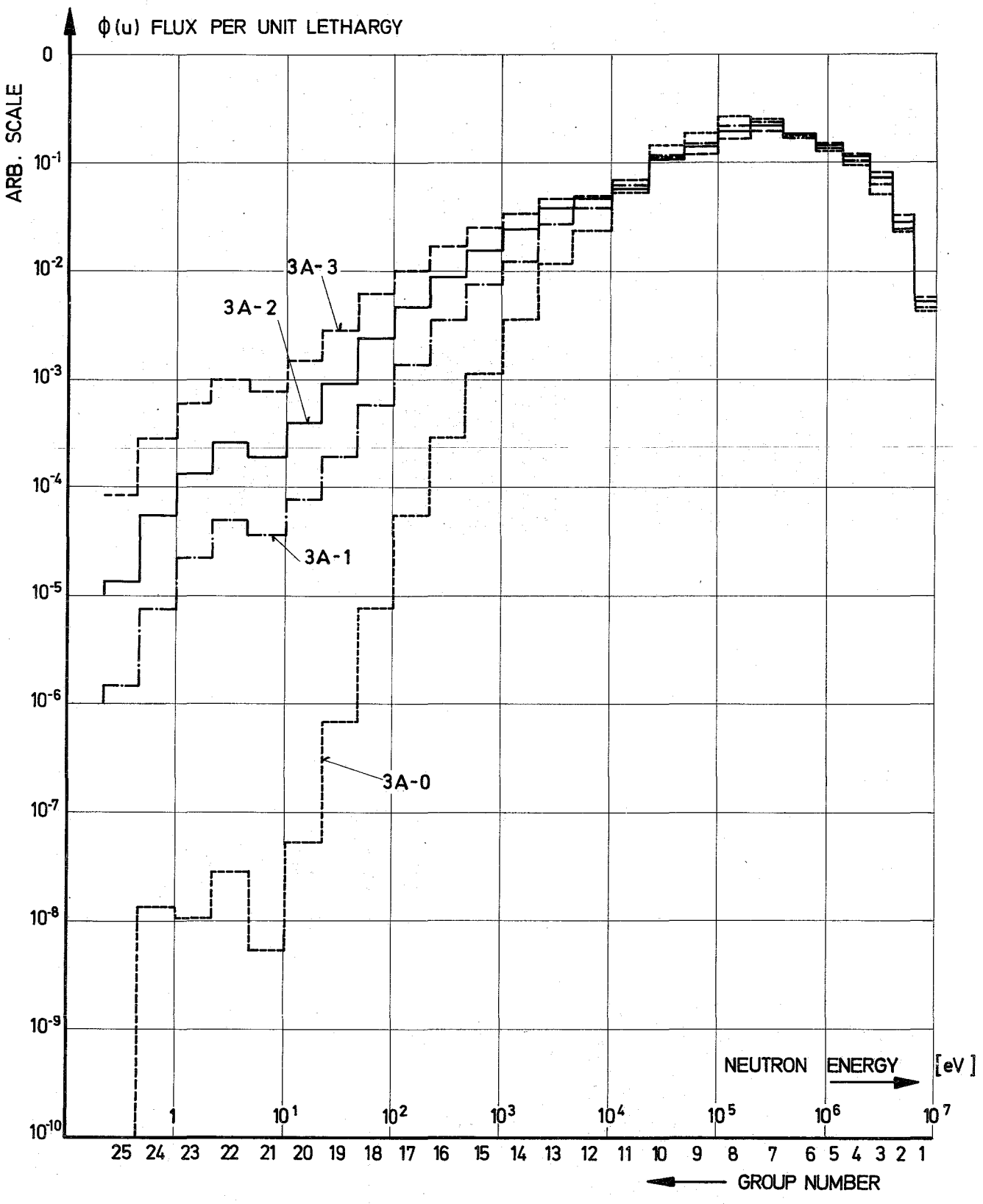

FIG. 1 NEUTRON SPECTRA AT THE CORE CENTER OF 3A ASSEMBLIES, CALCULATED WITH NORMAL SNEAK SET

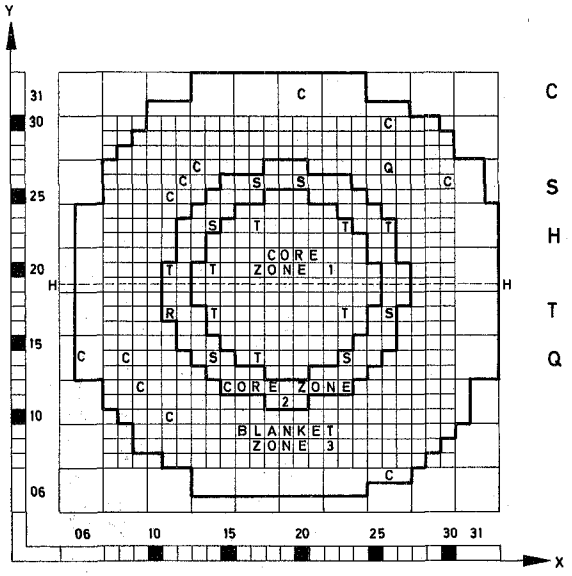

C ELEMENTS WITH MONITORING DETECTORS

S SAFETY RODS

H HORIZONTAL CHANNEL

T SHIM ROD

Q NEUTRON SOURCE

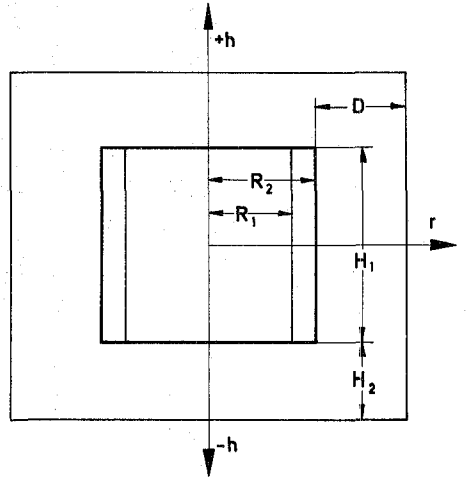

H_1 HEIGHT OF CORE ZONE 1 80.54 cm

H_2 HEIGHT OF AXIAL BLANKET 30.5 cm

R_1 RADIUS OF CORE ZONE 1 33.76 cm

R_2 RADIUS OF CORE ZONE 2 44.66 cm

D THICKNESS OF RADIAL BLANKET 36.2 cm

FIG. 2 CONFIGURATION AND DIMENSIONS OF SNEAK ASSEMBLY 3A-2

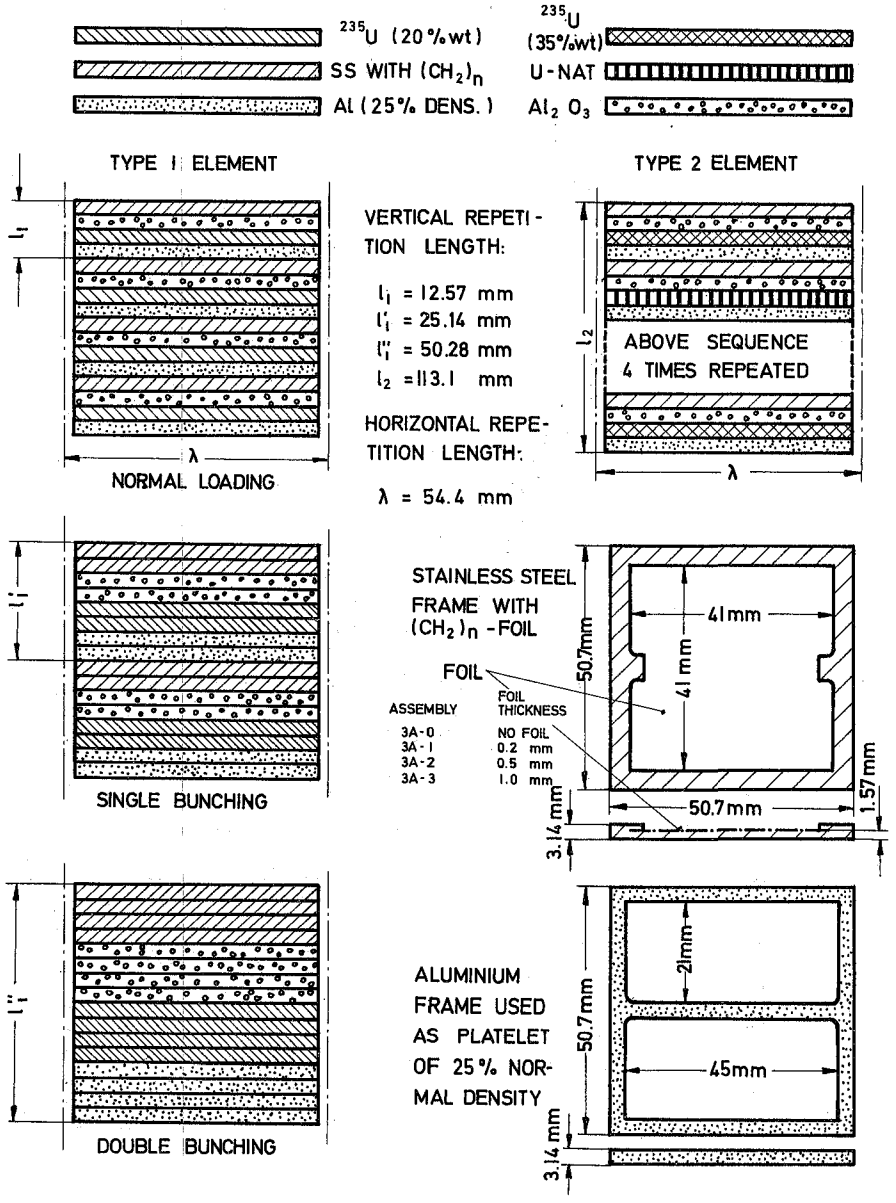

FIG. 3 CELL STRUCTURES AND SPECIAL PLATELETS USED IN SNEAK ASSEMBLIES 3A

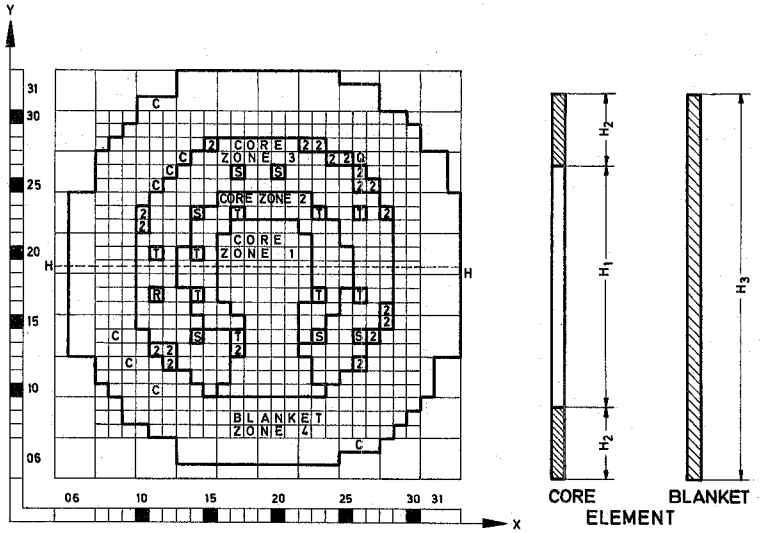

C ELEMENTS WITH MONITORING DETECTORS

S SAFETY RODS

T SHIM RODS

R CONTROL ROD

Q NEUTRON SOURCE

H HORIZONTAL CHANNEL

2 ZONE 2 TYPE ELEMENT AT CORE EDGE

H_1 = 80.54cm
H_2 = 30.50cm
H_3 = 141.54cm

ACTUAL CONFIGURATION

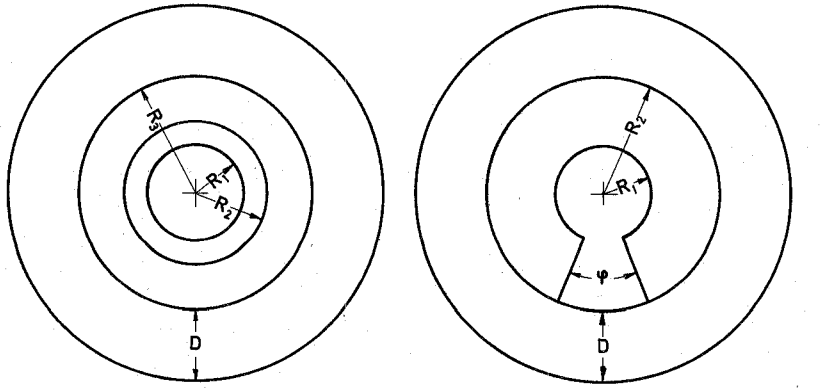

R_1 = 20.6 cm R_3 = 53.6 cm
R_2 = 33.0 cm D = 27.3 cm

R_1 = 20.6 cm $\varphi = \frac{\pi}{4}$ (STEP 4)
R_2 = 51.3 cm D = 30.0 cm

CONFIGURATION USED FOR
1 DIM. CALCULATIONS 2 DIM. CALCULATIONS

FIG. 4 CONFIGURATIONS AND DIMENSIONS OF SNEAK ASS. 3A-0

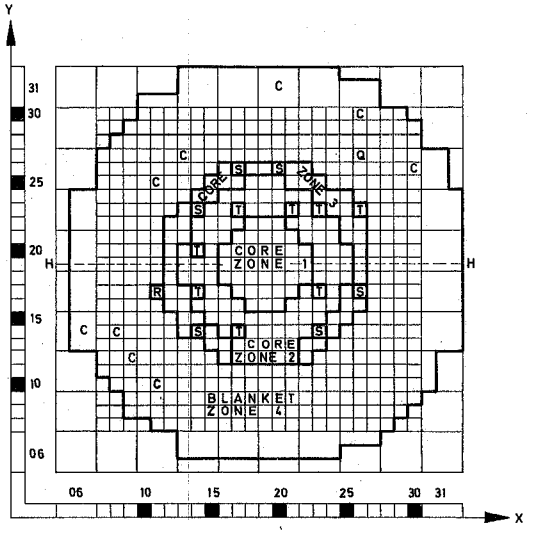

C ELEMENTS WITH MONITORING DETECTORS

S SAFETY RODS

H HORIZONTAL CHANNEL

T SHIM RODS

R CONTROL ROD

Q NEUTRON SOURCE

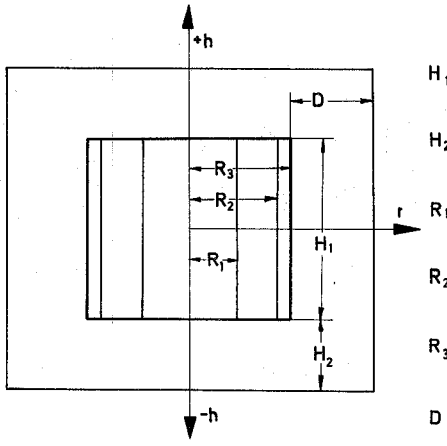

H_1 HEIGHT OF CORE ZONE 1 80.54 cm

H_2 HEIGHT OF AXIAL BLANKET 30.5 cm

R_1 RADIUS OF CORE ZONE 1 18.7 cm

R_2 RADIUS OF CORE ZONE 2 34.8 cm

R_3 RADIUS OF CORE ZONE 3 42.2 cm

D THICKNESS OF RADIAL BLANKET 38.7 cm

FIG. 5 CONFIGURATION AND DIMENSIONS OF SNEAK ASSEMBLY 3A-3

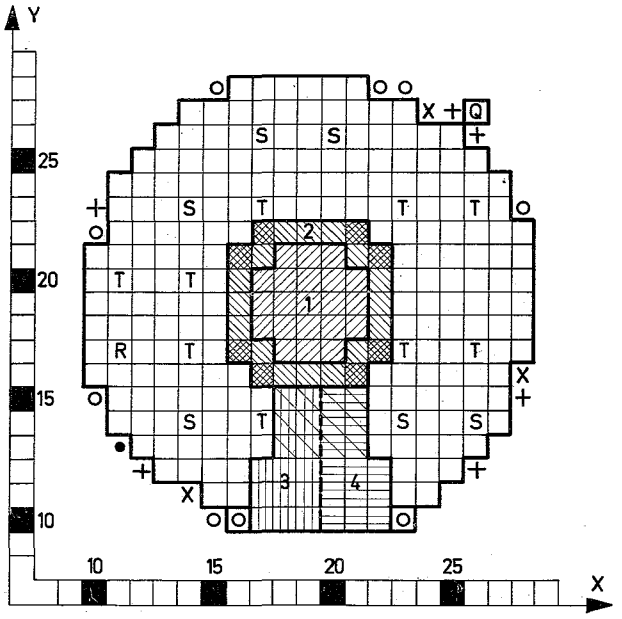

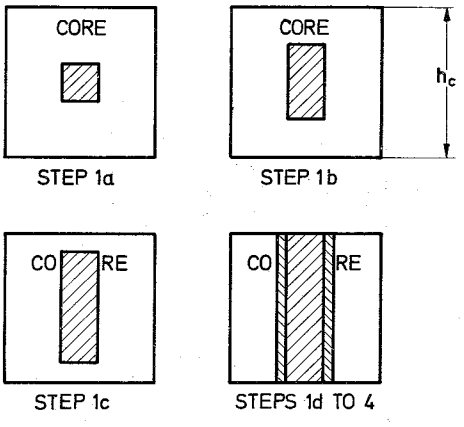

FIG. 6 VOID EXPERIMENT IN SNEAK ASSEMBLY 3A-1 (STEP 4 LEADS TO ASSEMBLY 3A-0)

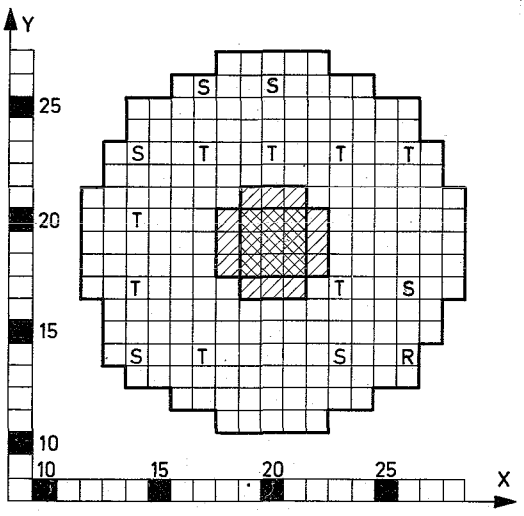

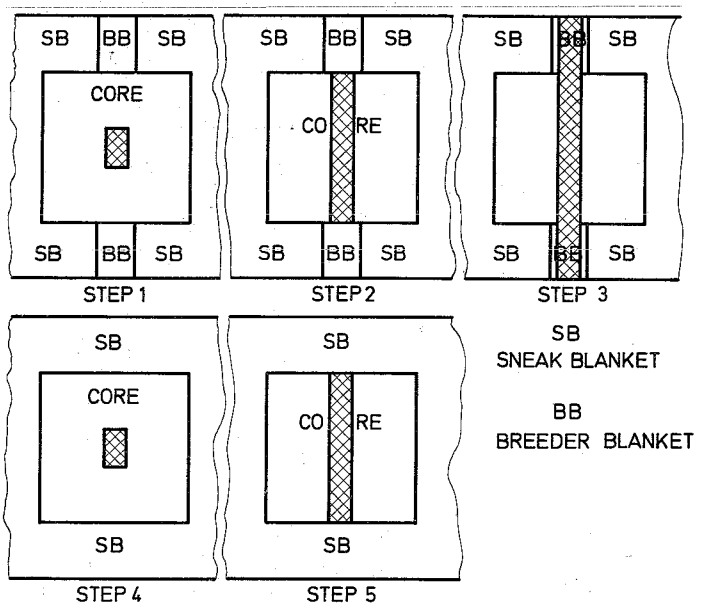

FIG. 7 VOID EXPERIMENT IN SNEAK ASSEMBLY 3A-2

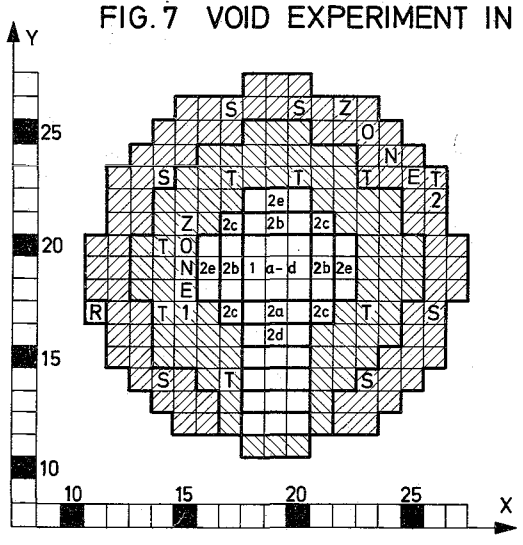

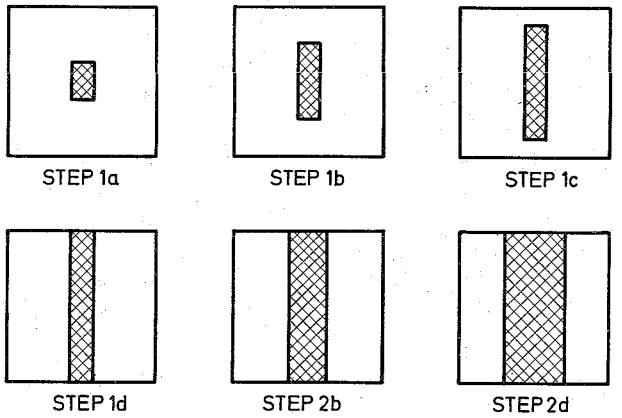

FIG. 8 FLOODING EXPERIMENT IN SNEAK ASSEMBLY 3A-2

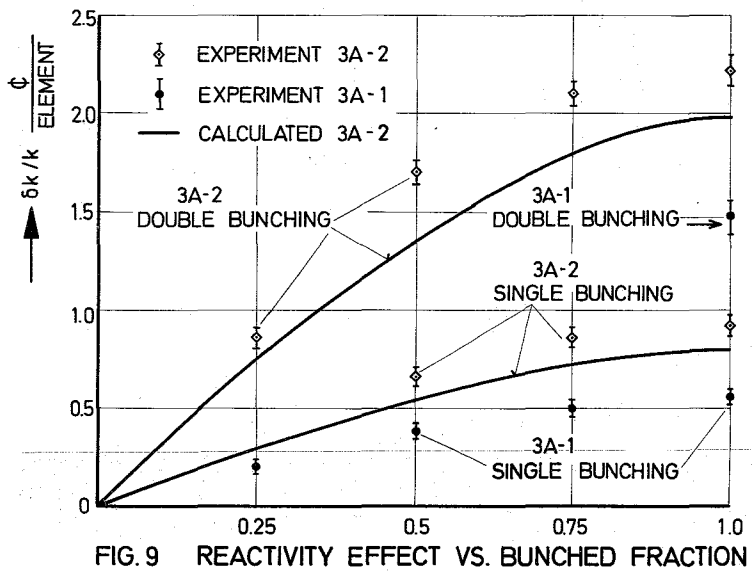

FIG. 9 REACTIVITY EFFECT VS. BUNCHED FRACTION OF CORE HEIGHT

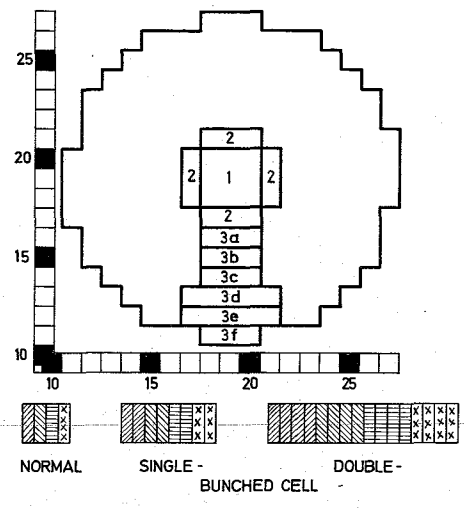

FIG. 10 LOCATION OF FUEL ELEMENTS FOR HETEROGENEITY EXPERIMENTS IN SNEAK ASS. 3A-2

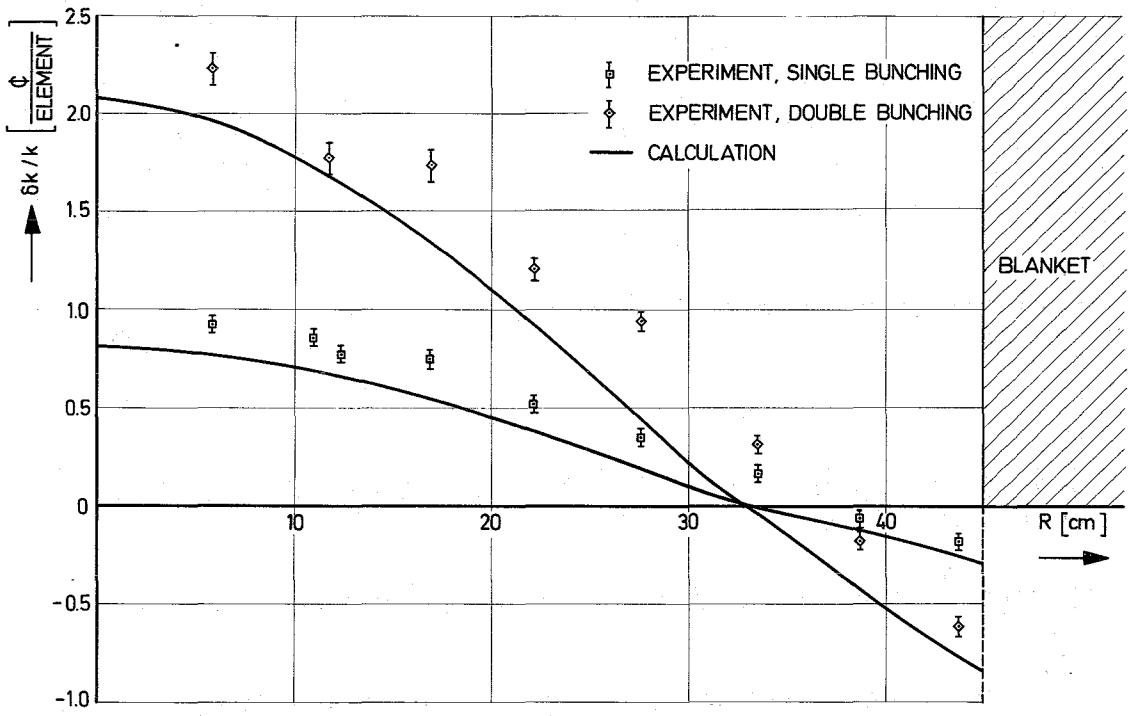

FIG. 11 REACTIVITY EFFECT DUE TO BUNCHING OF CORE CELLS IN SNEAK 3A-2 VS. RADIAL POSITION OF BUNCHED ELEMENTS

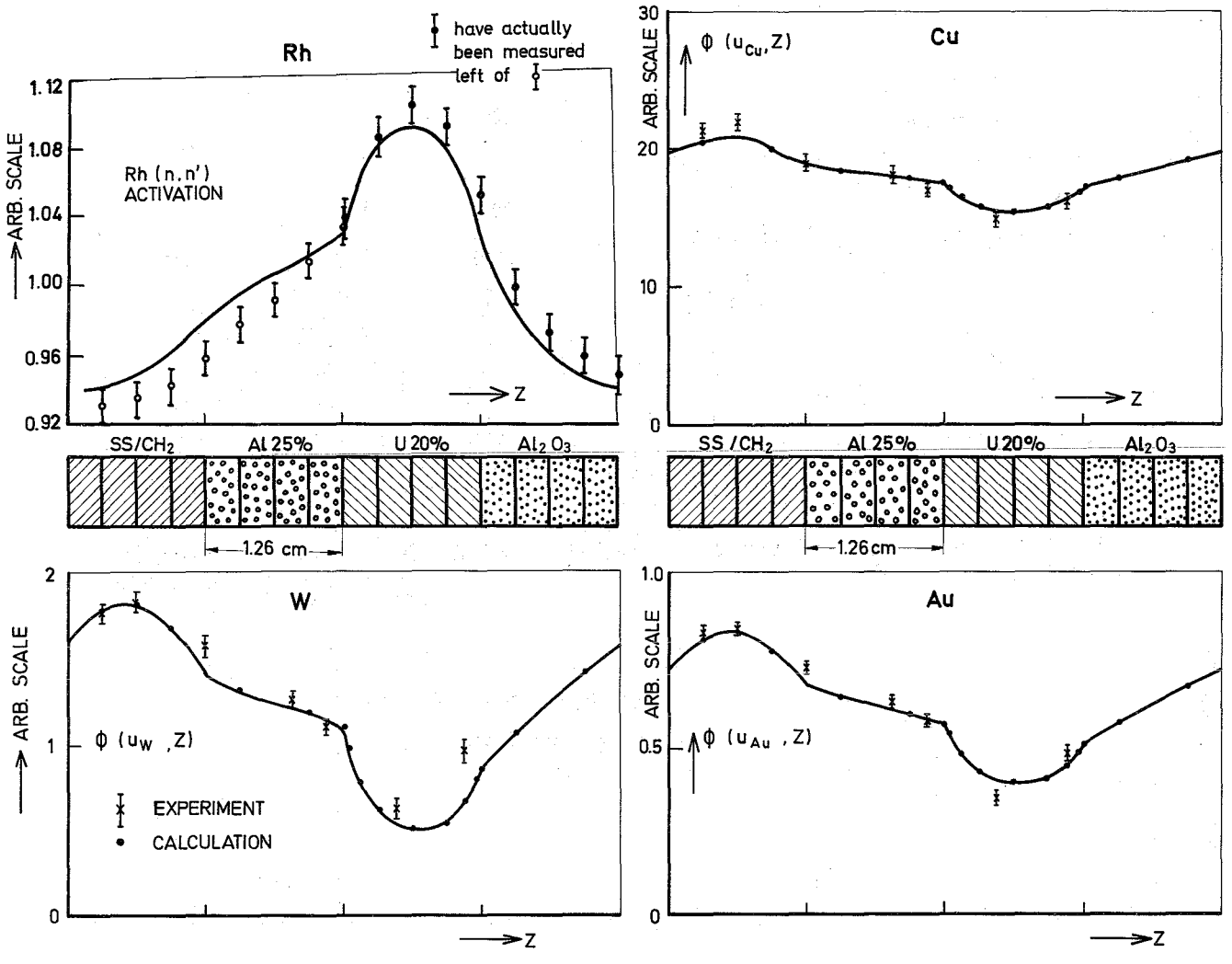

FIG. 12 FLUX FINE STRUCTURE ACROSS THE UNIT CELL OF SNEAK-ASSEMBLY 3A-2 (DOUBLE-BUNCHED).

THE VALUES RELATED TO Cu, W AND Au ARE TO THE SAME ARBITRARY FLUX SCALE

THE SMOOTH CURVES ARE DRAWN THROUGH THE CALCULATED VALUES

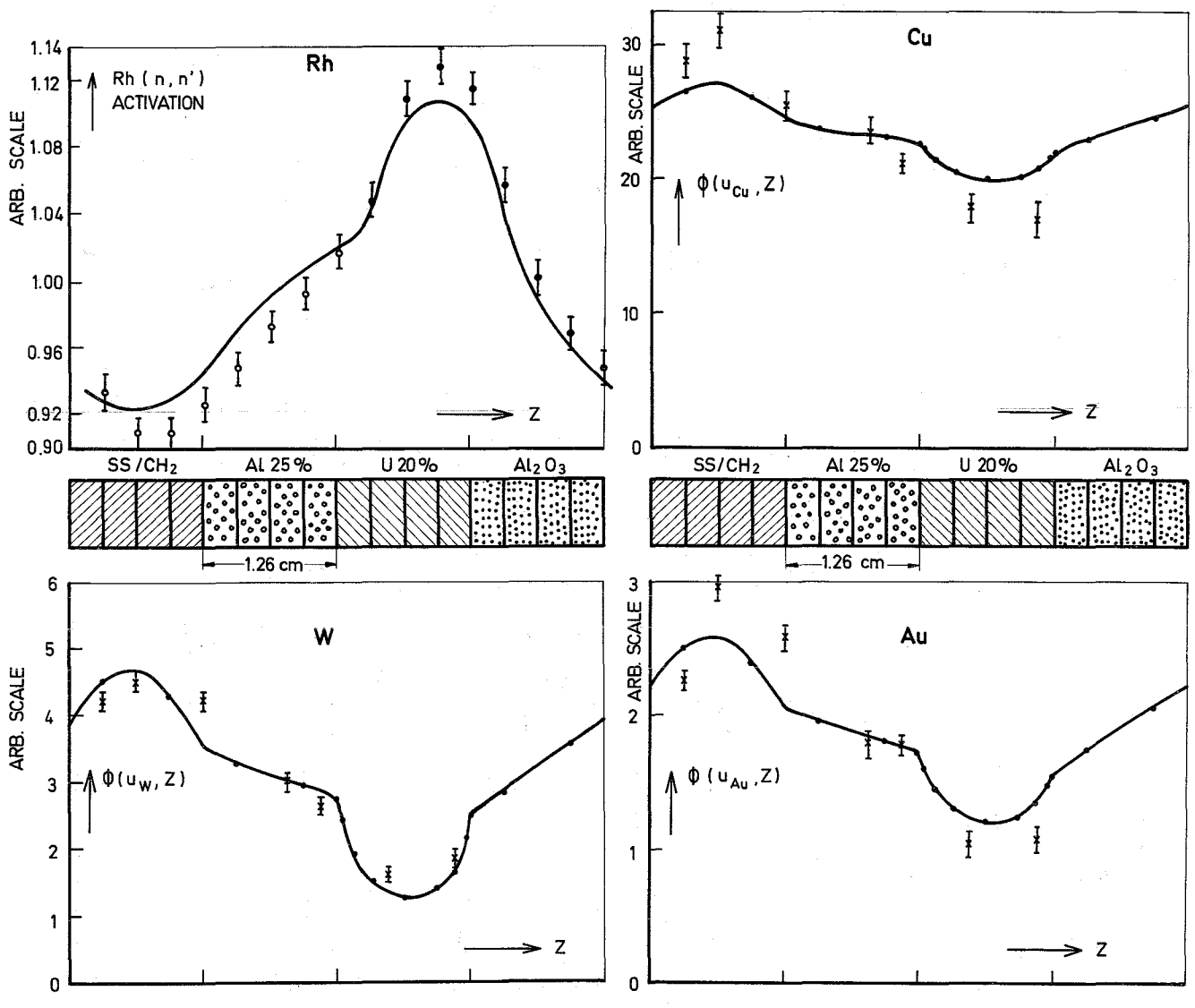

FIG. 13 FLUX FINE STRUCTURE ACROSS THE UNIT CELL OF SNEAK - ASSEMBLY 3A-3 (DOUBLE - BUNCHED)

THE VALUES RELATED TO Cu, W AND Au ARE TO THE SAME ARBITRARY FLUX SCALE

THE SMOOTH CURVES ARE DRAWN THROUGH THE CALCULATED VALUES

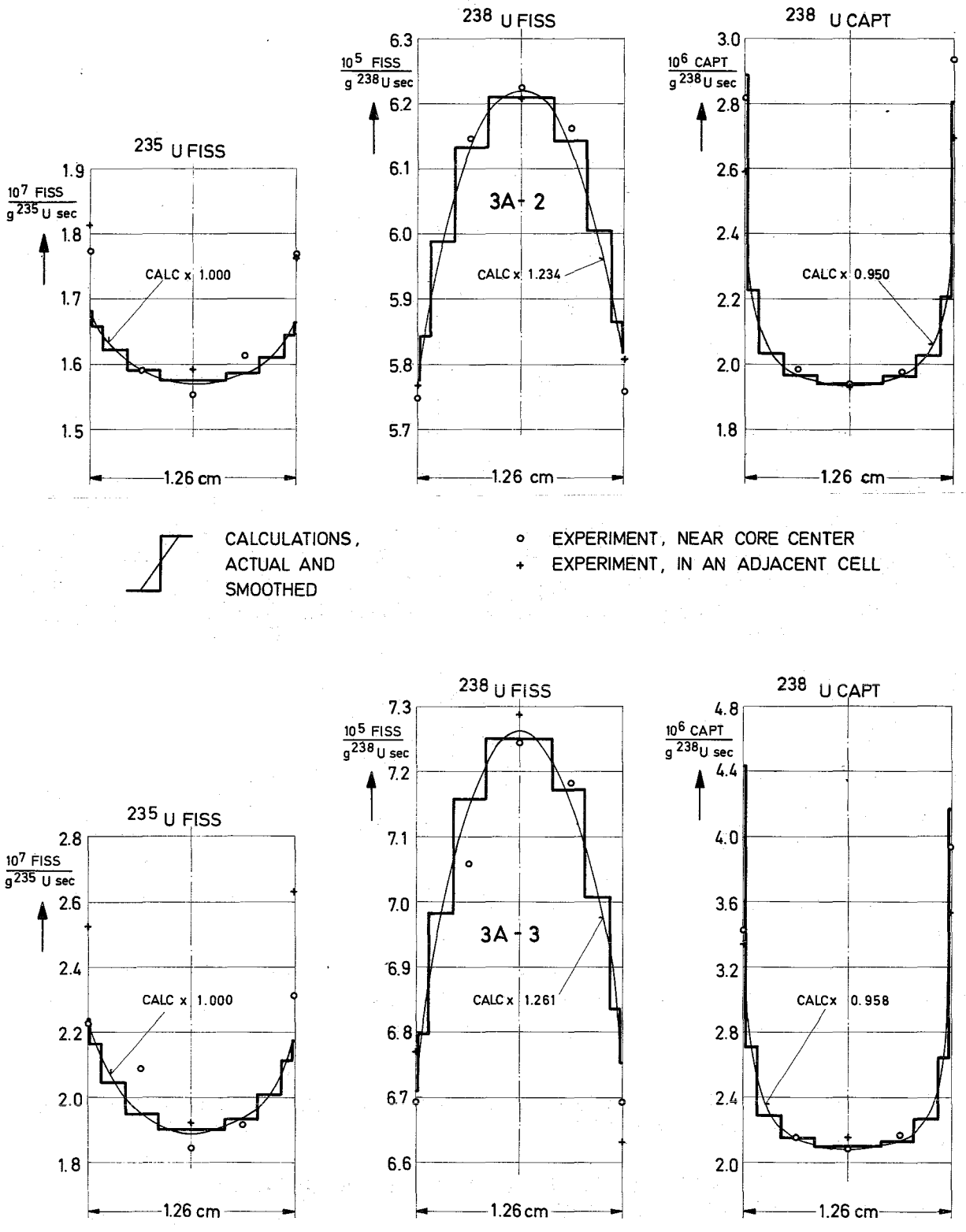

FIG. 14 COMPARISON OF EXPERIMENTAL AND CALCULATED LOCAL VARIATION OF REACTION RATES WITHIN THE FUEL ZONE (20% ENRICHED URANIUM) OF SNEAK-ASSEMBLIES 3A-2 (UPPER GRAPHS) AND 3A-3 (LOWER GRAPHS). THE CALCULATIONS ARE BASED ON THE SNEAK SET.

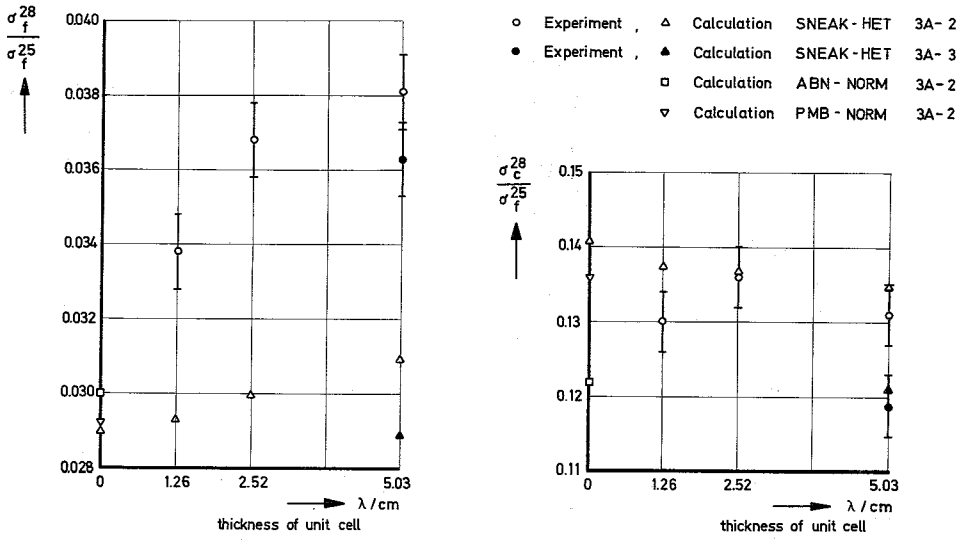

Fig. 15 Central Reaction Rate Ratios in SNEAK Assemblies for Different Degrees of Bunching

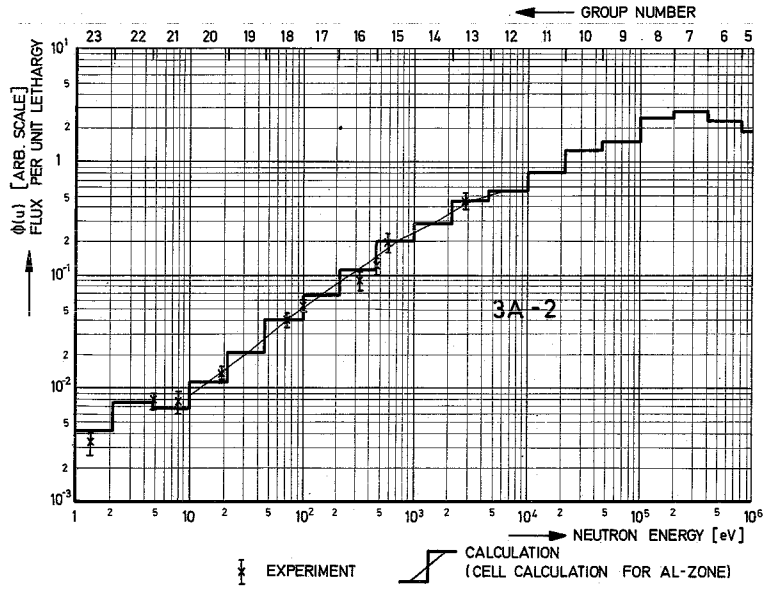

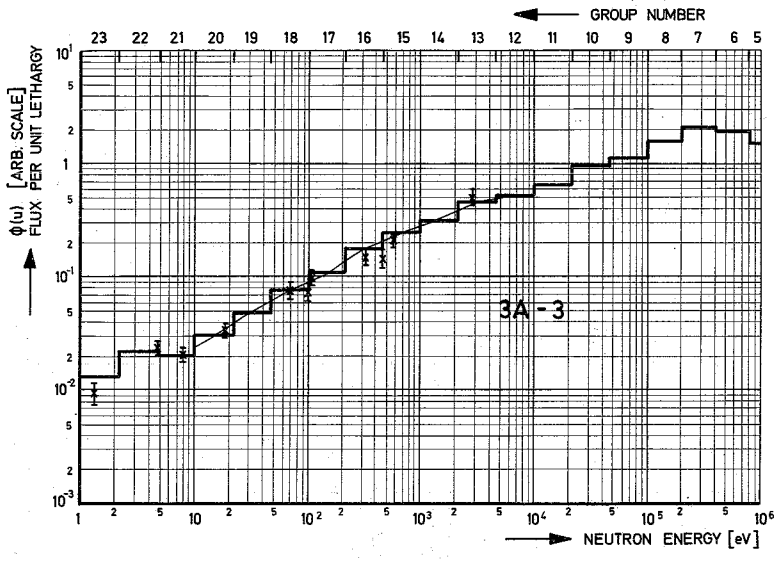

FIG. 16 EXPERIMENTAL AND CALCULATED SPECTRUM IN THE CENTERS OF THE DOUBLE BUNCHED CORES OF ASSEMBLIES 3A-2 AND 3A-3

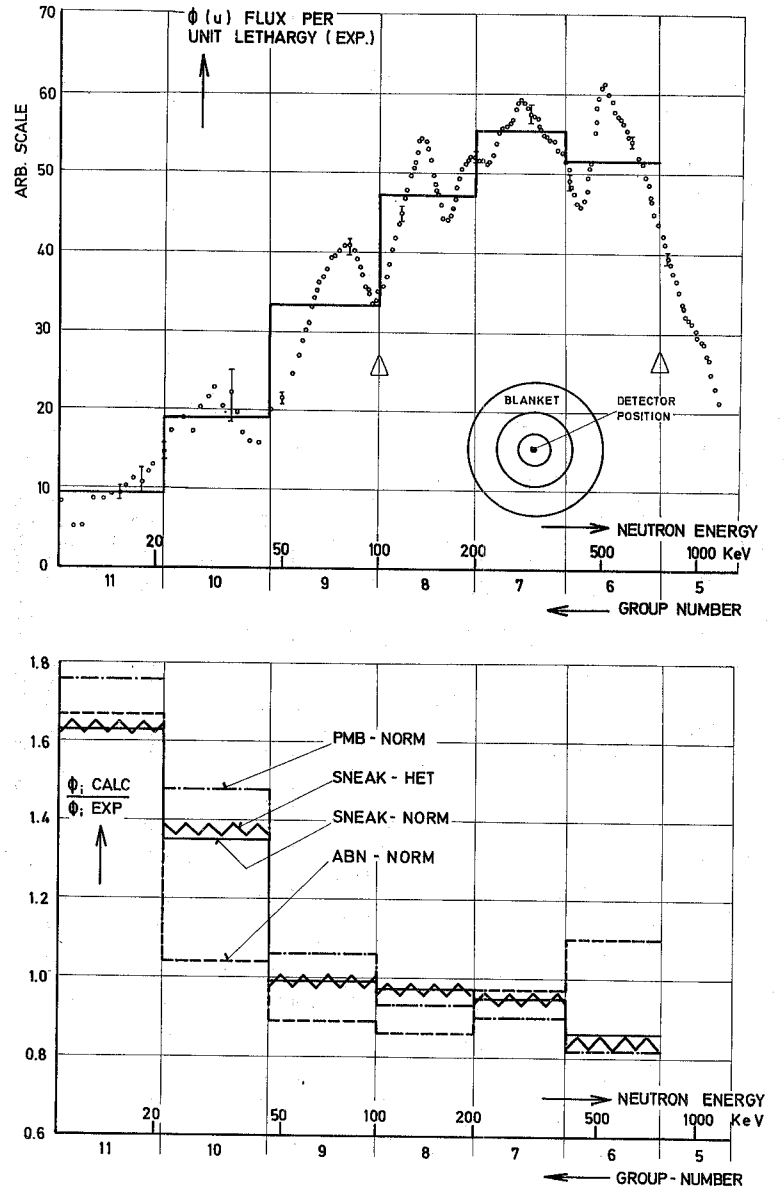

FIG. 17 COMPARISON BETWEEN CALCULATED AND MEASURED NEUTRON SPECTRUM AT THE CORE CENTER OF SNEAK 3A-2 (POS. 19 I 20)

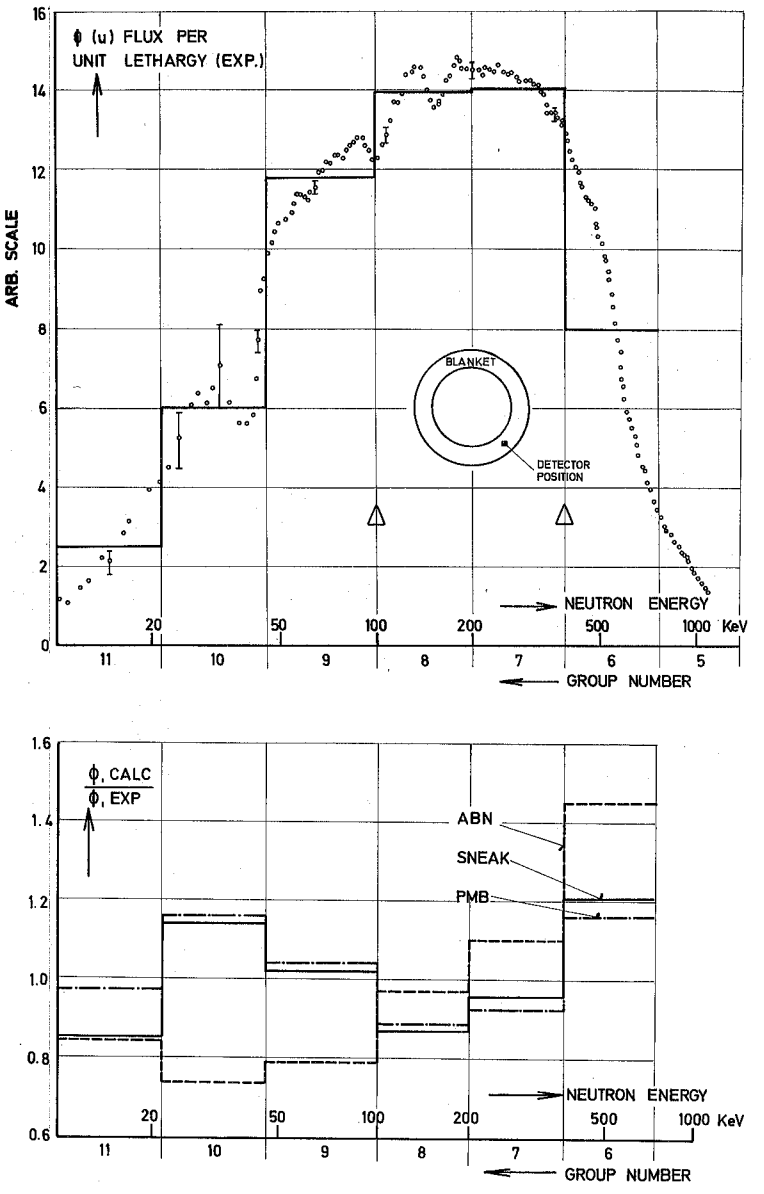

FIG. 18 COMPARISON BETWEEN CALCULATED AND MEASURED NEUTRON SPECTRUM IN THE BLANKET OF SNEAK ASSEMBLY 3A-2 (POS. 06 I 10)

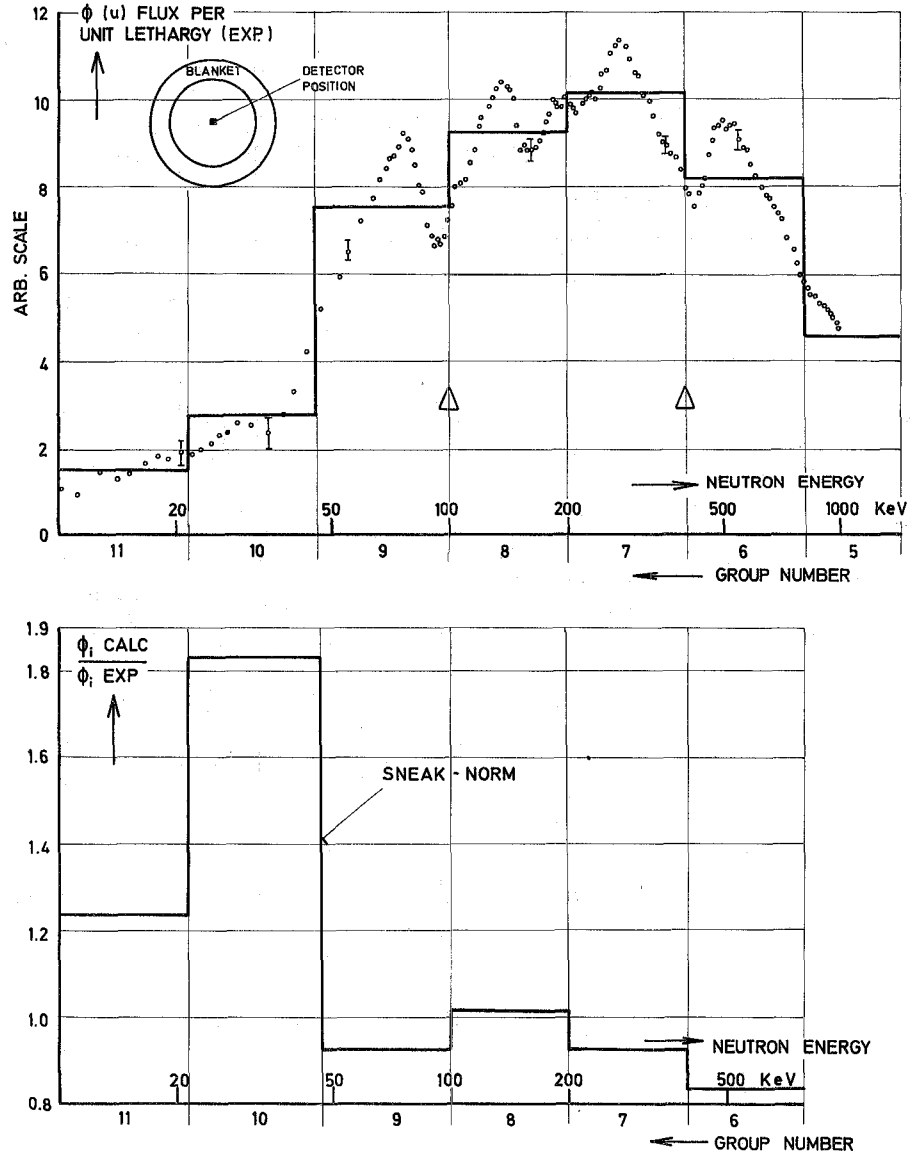

FIG. 19 COMPARISON OF MEASURED AND CALCULATED NEUTRON SPECTRA AT THE CENTER OF SNEAK 3A-0 (POS. 19 I 19)

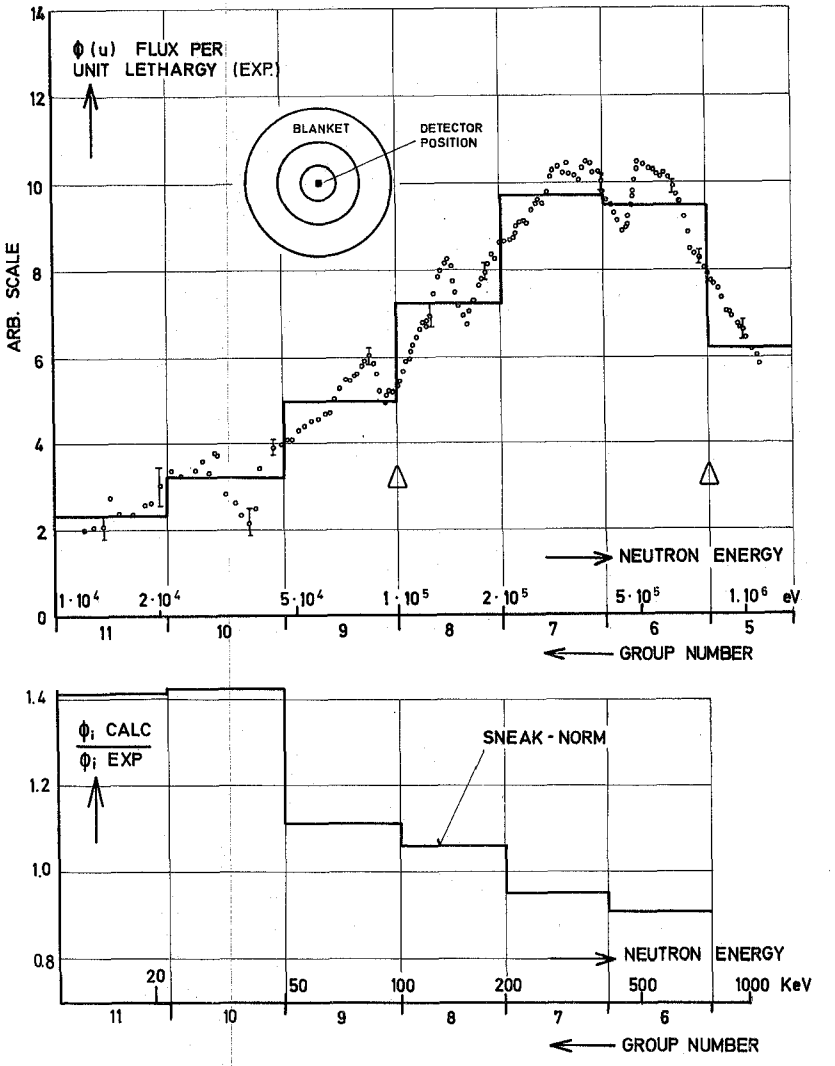

FIG. 20 NEUTRON SPECTRA AT THE CORE CENTER OF SNEAK ASSEMBLY 3A-3 POS. (19 I 19)

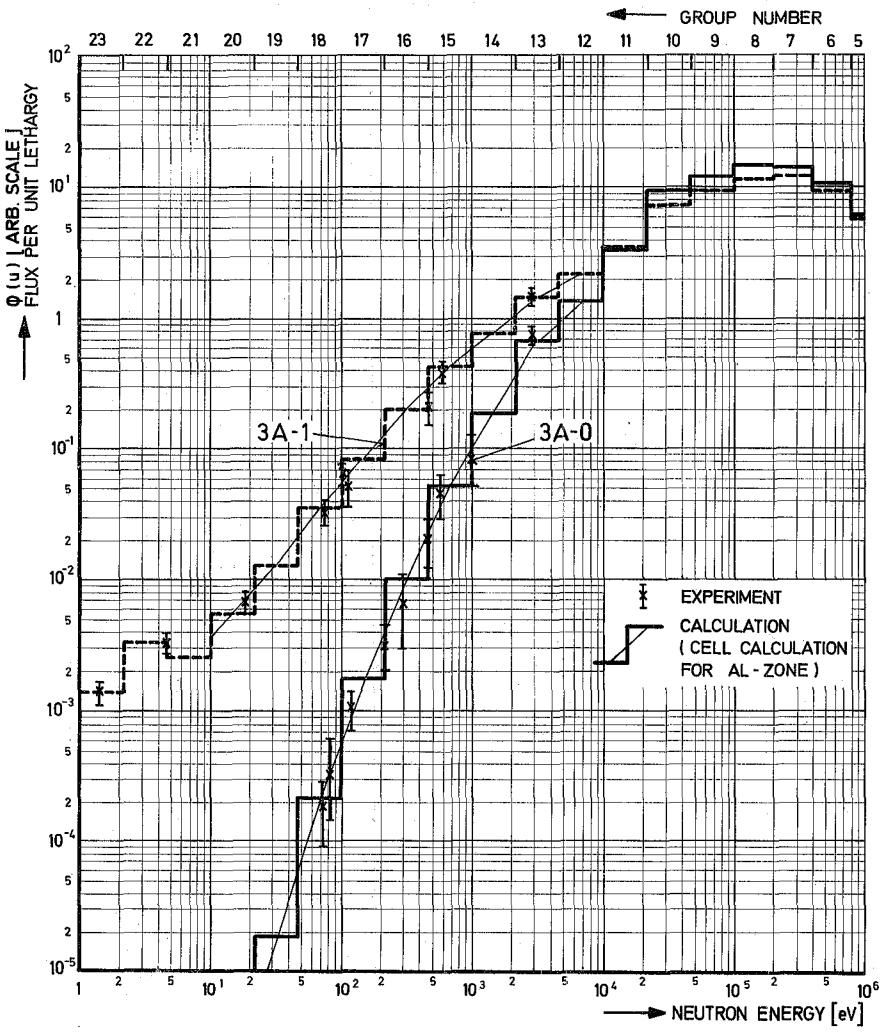

FIG. 21 EXPERIMENTAL AND CALCULATED SPECTRA IN THE CENTER OF SNEAK ASSEMBLIES 3A-0 AND 3A-1

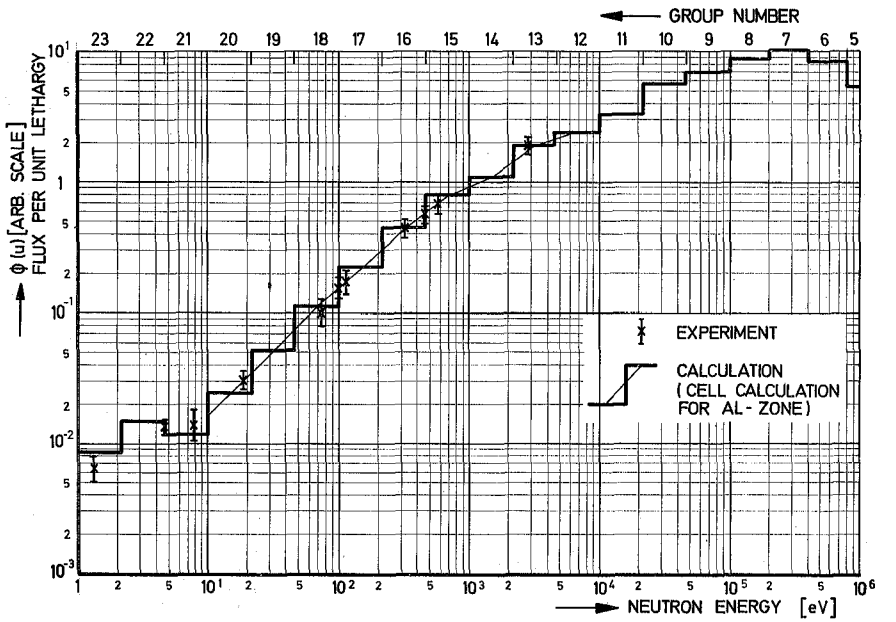

FIG. 22 EXPERIMENTAL AND CALCULATED SPECTRUM IN THE CENTER OF SNEAK ASSEMBLY 3A-2

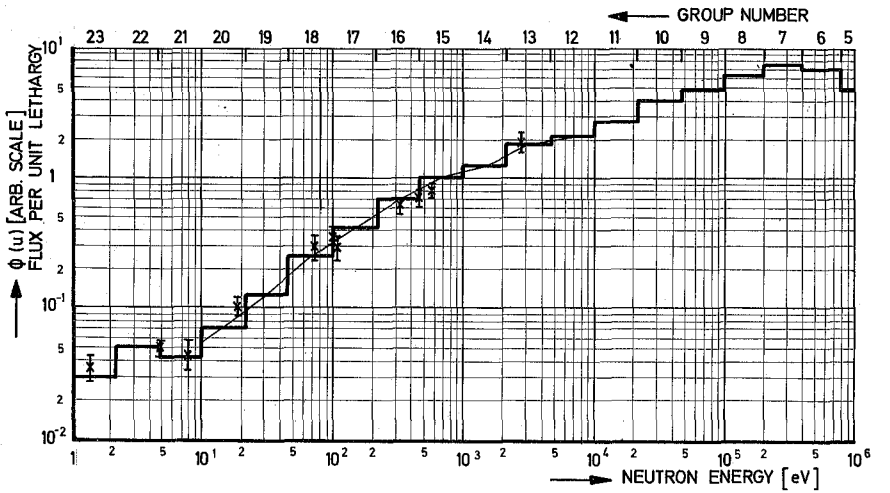

FIG. 23 EXPERIMENTAL AND CALCULATED SPECTRUM IN THE CENTER OF SNEAK ASSEMBLY 3A-3

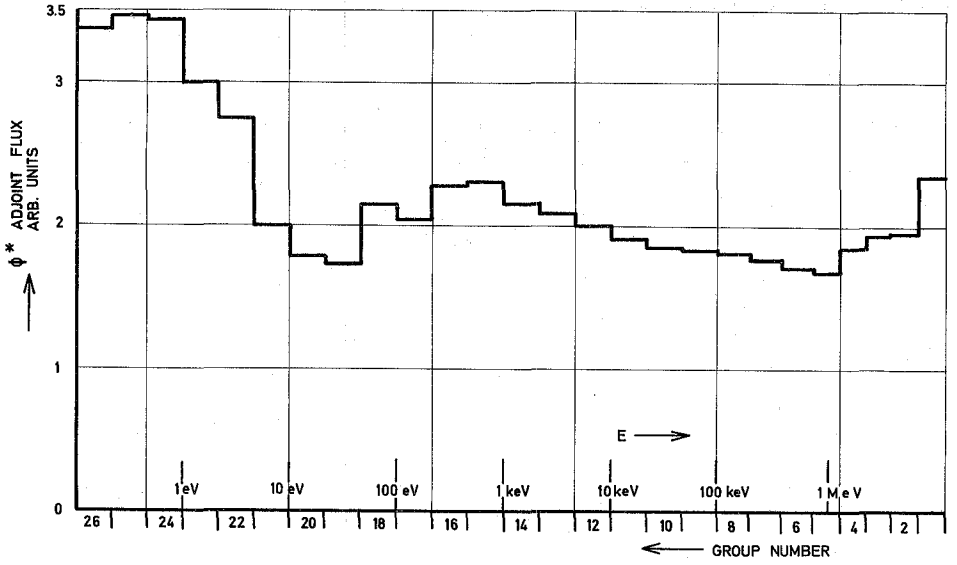

FIG. 24 CALCULATED ADJOINT FLUX AT THE CENTER OF SNEAK ASSEMBLY 3A - 2 (SNEAK - HET)

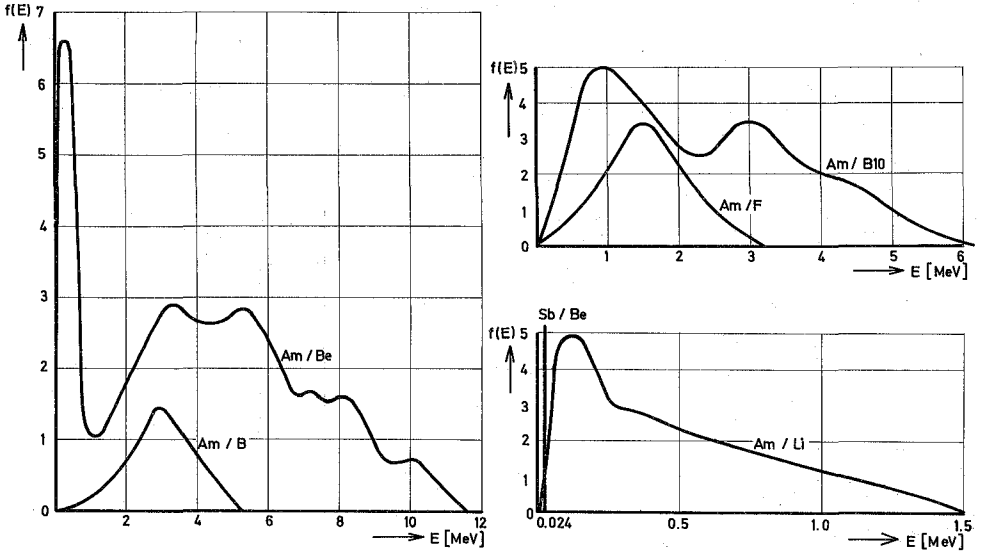

FIG. 25 NEUTRON SOURCE SPECTRA USED

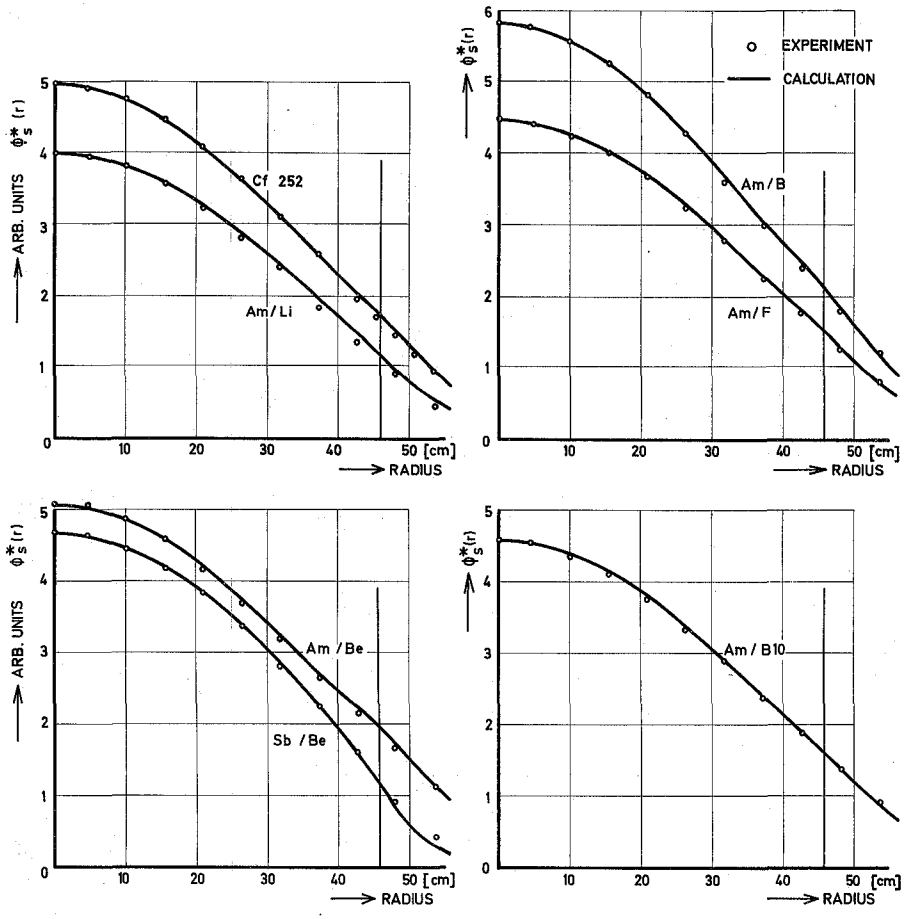

FIG. 26 COMPARISON OF MEASURED AND CALCULATED RADIAL IMPORTANCE DISTRIBUTION $\phi_s^*(r)$ FOR NEUTRONS OF THE VARIOUS SOURCES FOR SNEAK-ASSEMBLY 3A - 2

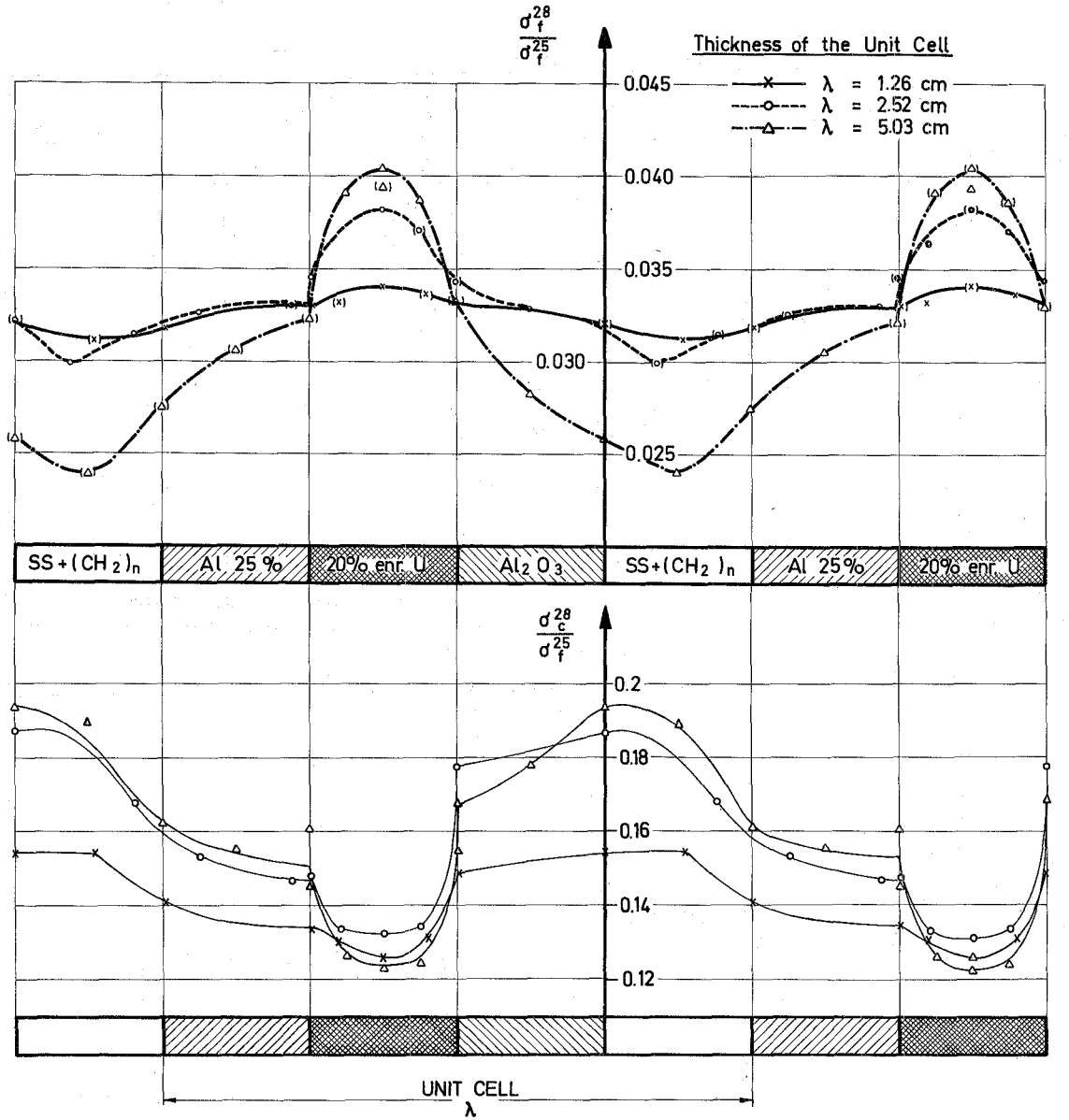

FIG. 27 $\frac{\sigma_f^{28}}{\sigma_f^{25}}$ AND $\frac{\sigma_c^{28}}{\sigma_f^{25}}$ IN ASSEMBLY 3A-2 FOR THREE DEGREES OF BUNCHING

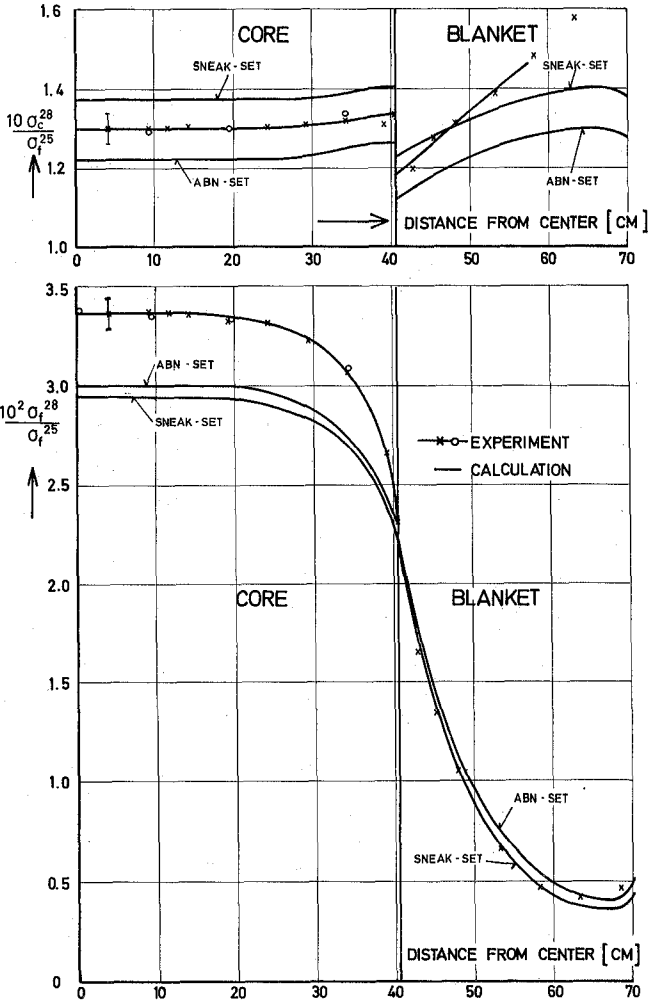

FIG. 28 COMPARISON OF MEASURED AND CALCULATED REACTION RATE RATIOS ALONG THE CORE AXIS IN SNEAK ASSEMBLY 3A-2

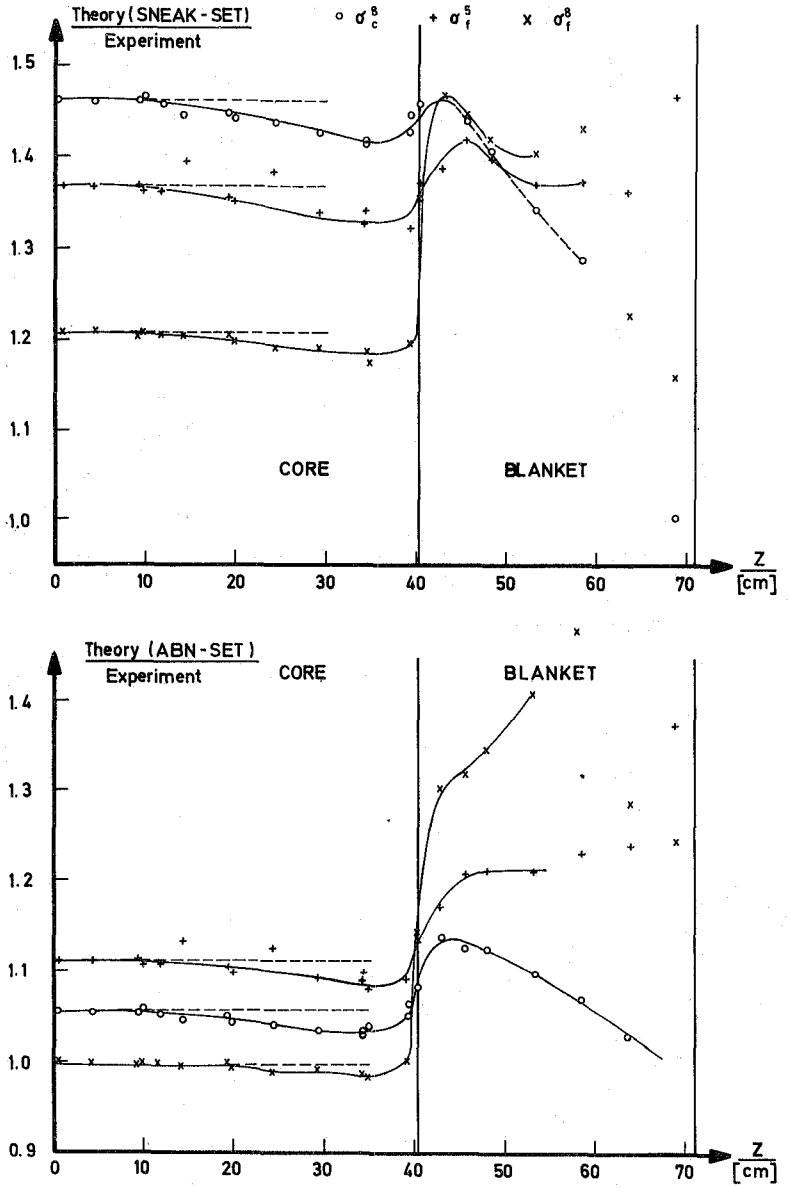

FIG. 29 THE RATIO OF CALCULATED TO MEASURED REACTION RATES ALONG THE CENTRAL REACTOR AXIS

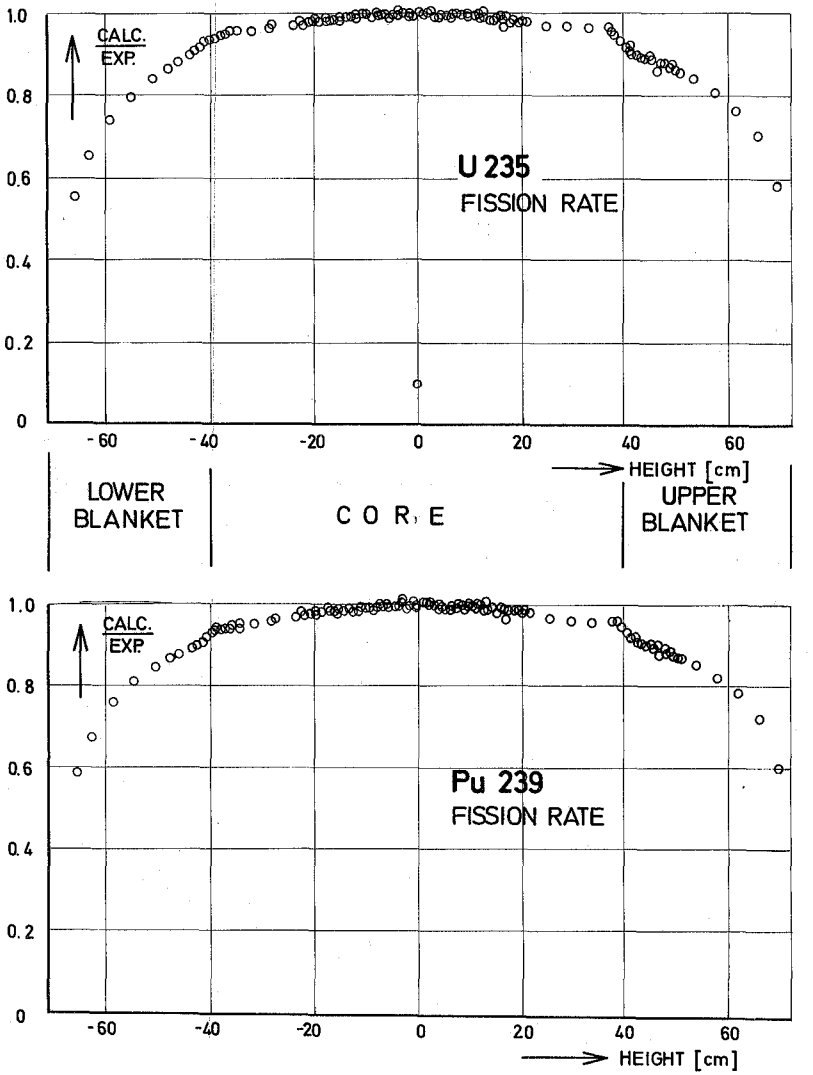

FIG. 30 RATIO OF CALCULATED TO EXPERIMENTAL FISSION RATES OF U 235 AND Pu 239 (NORMALIZED AT THE CENTER) FOR SNEAK-ASSEMBLY 3A-2. (CHAMBER TRAVERSES.)

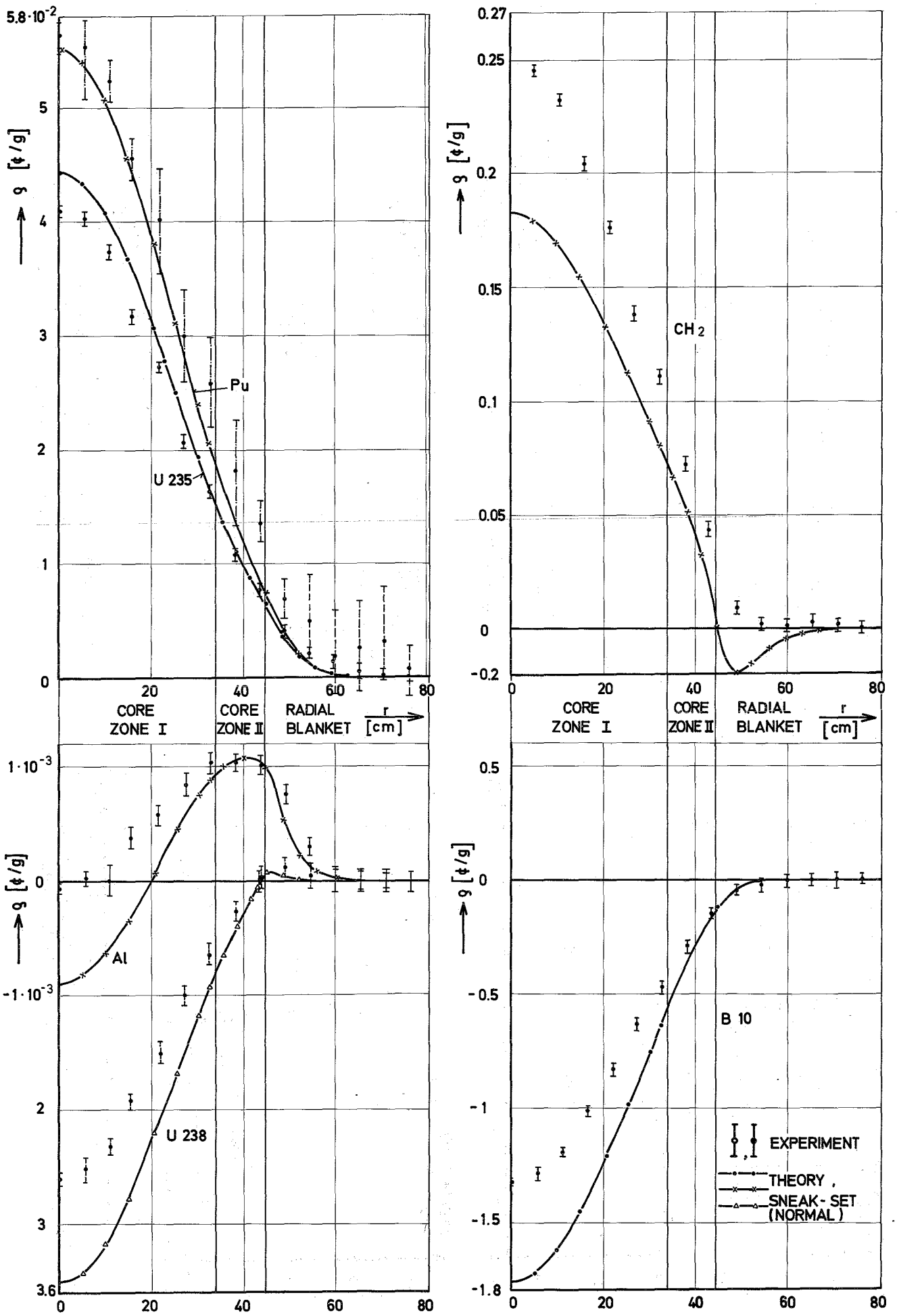

FIG. 31 RADIAL REACTIVITY TRAVERSES OF DIFFERENT MATERIALS IN SNEAK ASSEMBLY 3A-2

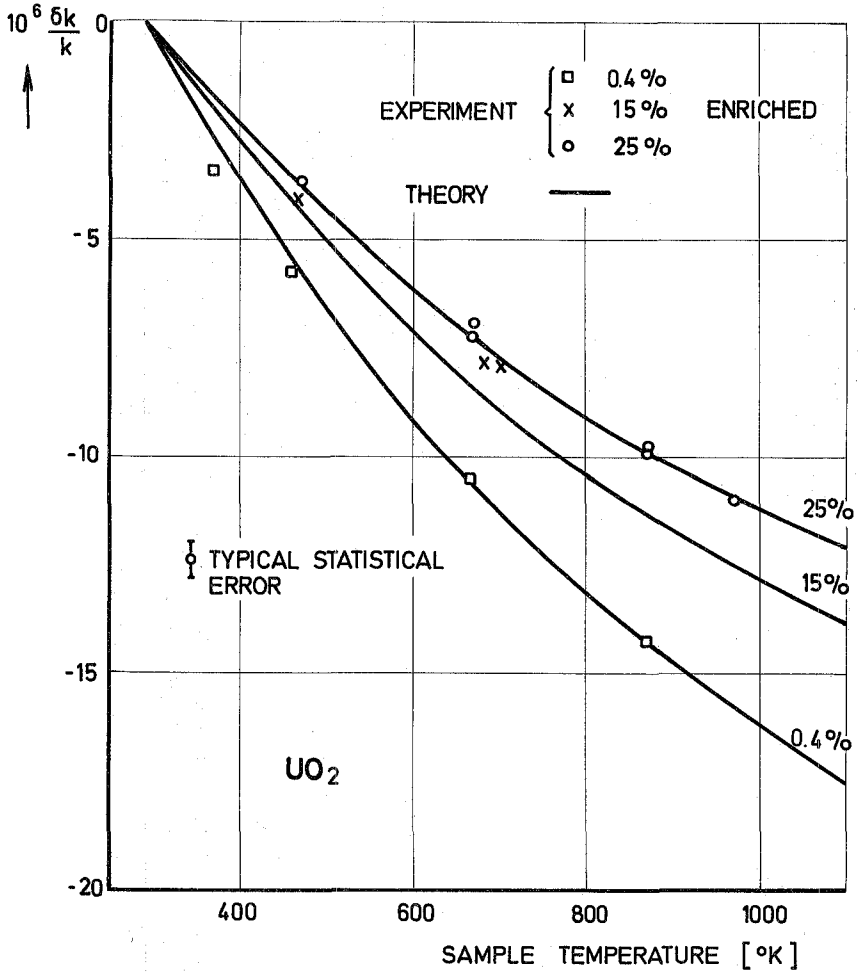

FIG. 32 TEMPERATURE DEPENDENT REACTIVITY EFFECT OF URANIUM OXIDE DOPPLER SAMPLES IN ASSEMBLY 3A-2

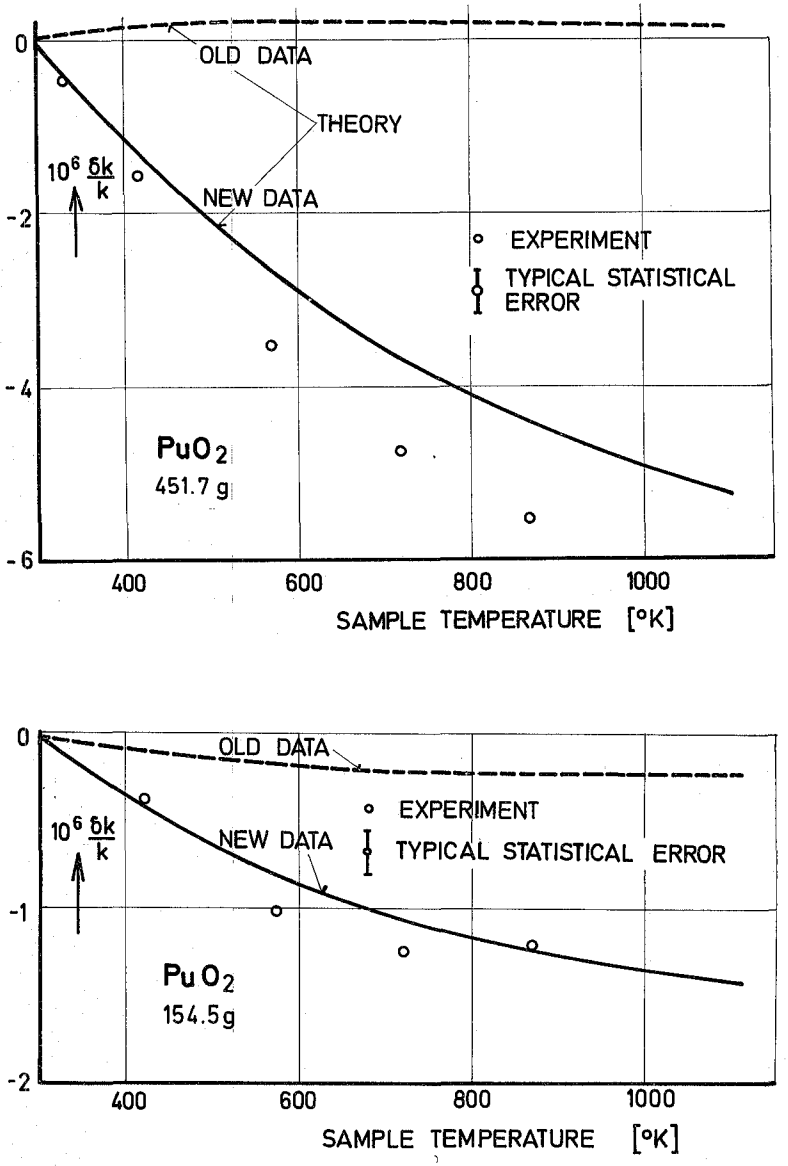

FIG. 33 TEMPERATURE DEPENDENT REACTIVITY EFFECT OF PLUTONIUM OXIDE SAMPLES IN ASSEMBLY 3A-2

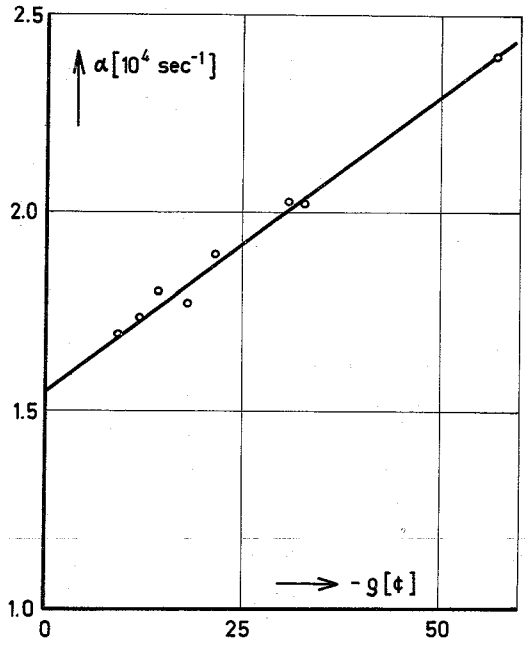

FIG. 34 α AS A FUNCTION OF NEGATIVE REACTIVITY FOR THE ROSSI - α EXP. ON SNEAK - ASSEMBLY 3A - 2

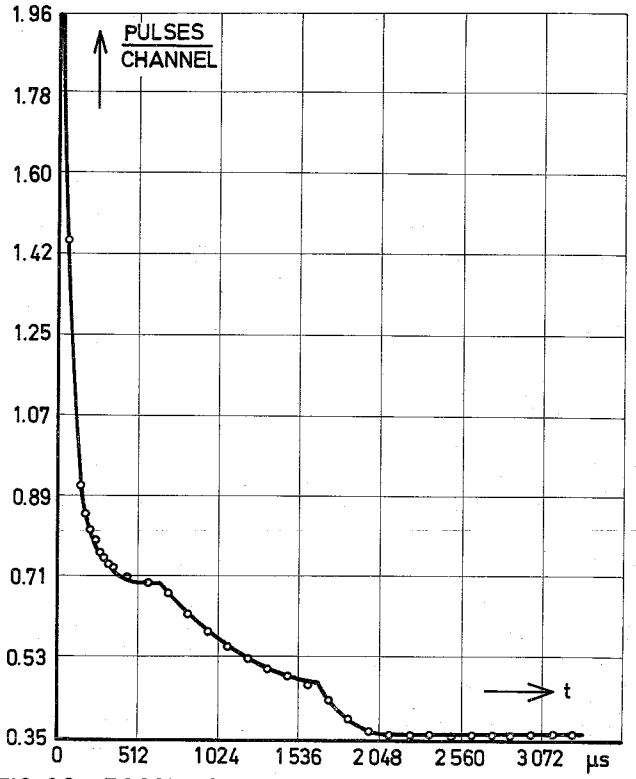

FIG. 36 ROSSI - α CORRELATION FUNCTION FOR SNEAK - ASSEMBLY 3A-3, (ABOUT 1 $ SUBCRITICAL)

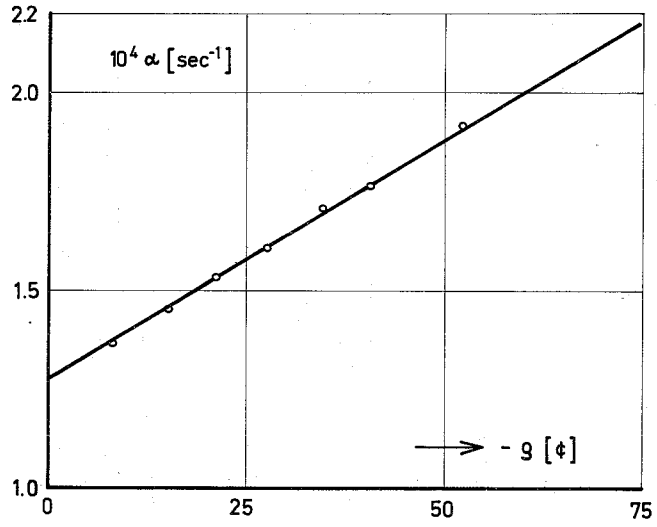

FIG. 35 α AS A FUNCTION OF NEGATIVE REACTIVITY FOR THE PULSED SOURCE EXPERIMENT ON SNEAK - ASSEMBLY 3A - 3

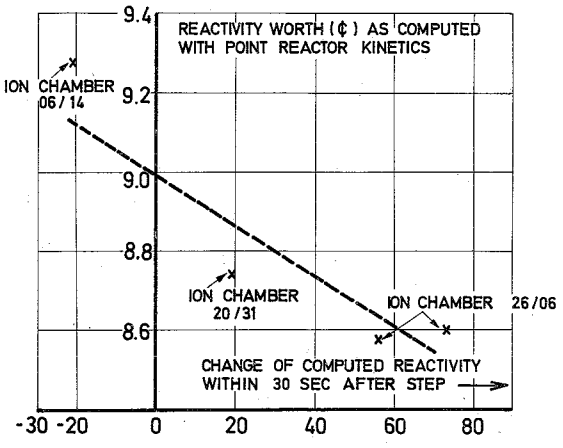

FIG. 37 DEMONSTRATION OF INTER - POLATION METHOD FOR SHIM ROD T 09